Similarity techniques in the theory of the FEL amplifier

E. L. Saldin and E. A. Schneĭdmiller
Scientific and Industrial Union of Automated Systems, Samara

M. V. Yurkov
Joint Institute for Nuclear Research, Dubna

Fiz. Elem. Chastits At. Yadra **23**, 239–294 (January–February 1992)

Problems related to the calculation of the FEL-amplifier output characteristics in the saturation regime are discussed. The optimization of the FEL-amplifier efficiency by variation of the undulator parameters is investigated. A scheme for calculating the optimal undulator parameters is described, and the output characteristics of the FEL amplifier with optimal undulator are given. The proposed computational schemes are based on the use of similarity techniques and the results of numerical modeling, which are represented as universal plots. The mathematical model of processes occurring in FEL amplifiers used in the numerical modeling takes into account factors such as the space charge and the energy spread of the beam particles. The rigorous results of the linear theory of the FEL amplifier are used as the standard for testing the numerical-modeling programs. A large number of universal plots which can be used directly for developing and designing FEL amplifiers are given.

INTRODUCTION

This study is devoted to the systematical exposition of the applications of similarity techniques in the linear and nonlinear theories of the FEL amplifier.[1)] This technique is used to transform absolute variables into relative ones. At the same time the parameters of the problem are combined into dimensionless power-law combinations, the similarity criteria. These similarity criteria are the only parameters of the problem, which has been reduced to dimensionless form. There is a dimensionless criterion corresponding to every factor influencing the operation of the FEL amplifier (the space charge, the energy spread, and so on). The similarity criterion for a given effect is a measure of its relative strength. If the situation is such that some effect becomes unimportant for the operation of the FEL amplifier, this is necessarily reflected in the corresponding selection criterion, which in that case takes small values and completely drops out of the set of arguments of the problem.

The advantages of using the similarity technique are obvious. A dimensional analysis of any problem, carried out before an analytic study, not only decreases the number of relevant independent terms, but makes it possible to systematize the grouping of the dimensional variables in the manner most convenient for further study. In the end, by solving dimensionless equations it becomes possible to represent the result of the study in a form such that its information content will simultaneously be very general and completely specific.

Similarity techniques have been widely used and very useful for disseminating concepts in the traditional area of ultrahigh-frequency electronics. However, these techniques are not yet as widely applied as they deserve to be in the physics of free-electron lasers. At the present time there seems to be a need for a text on this subject which would aid the experimentalist in the use of similarity techniques in practical applications of the FEL technique. The present study is an attempt to provide such a text which can to some degree prove useful to specialists.

Our basic goal is to instruct the reader how to obtain approximate results from dimensional analysis using a simplified model of the phenomenon in question. Such a quick way of estimating the FEL-amplifier parameters can prove very useful in injector and laboratory practice, particularly during the experimental design stage.

This review is short and does not deal with all aspects of the problem. For the sake of clarity we have restricted ourselves to the consideration of the one-dimensional approximation. The authors have made every effort to give a clear exposition. Therefore, almost all the results presented here are derived from first principles, and the reader can follow the derivation from beginning to end. The power of similarity techniques can also be demonstrated for models of a FEL amplifier in which diffraction of the radiation, the influence of the waveguide walls, etc., are taken into account. However, if we adhered to the detailed style of exposition that we have adopted, the description of the elementary model for these effects would drastically increase the size of this study. Therefore, to learn about such generalizations of the theory the reader should consult the original studies.

This study is organized as follows. In Sec. 1 we discuss the linear theory of the FEL amplifier. In our description of the linear theory, we focus on finding the analytic solutions of the self-consistent field equations, taking into account the influence of the space charge and the energy spread of the beam particles. The process by which the electron beam interacts with the electromagnetic wave in the undulator in the linear regime can be described by a single integro-differential equation. The solution of this equation for given initial conditions at the entrance to the interaction region makes it possible to determine the dependence of the amplitude of the wave field on the undu-

 0090-4759/92/010104-24$04.00

lator length and thereby to calculate the output characteristics of the FEL amplifier. The initial-value problem is solved by the Laplace-transform method. Our rigorous results, which are represented in normalized form, are used to find universal graphs which allow the output characteristics of the FEL amplifier to be calculated in the linear operating regime. In addition, our analytic solutions serve as a reliable basis for developing numerical methods. One area in which only numerical methods can be used is the analysis of nonlinear processes. It would be difficult to test numerical-modeling programs without using the rigorous results of the linear theory as a standard.

Similarity techniques play an important role in the numerical modeling of processes occurring in FEL amplifiers. In the one-dimensional approximation the output characteristics of the amplifier are determined by a system of eight dimensional parameters of the beam and undulator. The system of self-consistent field equations describing the interaction of the beam and the wave in the undulator can be formulated as a relation between dimensionless quantities. It follows from these equations that the set of similar operating regimes of the FEL amplifier is determined by the values of five dimensionless parameters. When the amplification factor is high, i.e., when the dimensionless undulator length is sufficiently large, the output amplitude of the field in the saturation regime is independent of the undulator length and the amplitude of the input signal. In this practically important case the maximum efficiency of the amplifier is a function of only three dimensionless parameters: the detuning parameter, the space-charge parameter, and the energy-spread parameter.

In Sec. 2 we present a scheme for calculating the output characteristics of the FEL amplifier in the saturation regime. This is the first presentation of such a scheme which is applicable for practical engineering. This scheme is based on the use of similarity techniques and numerical-modeling results, which are represented in the form of computational formulas and universal graphs. All the stages of numerical experiments are discussed: the physical formulation of the problem, the construction of a mathematical model of the amplifier, and the realization and actual calculation of the algorithm.

A promising method of raising the efficiency of FEL amplifiers is that of variation of the undulator parameters along its axis. This increases the amplifier efficiency to a factor of order unity. In Sec. 3 we discuss the further application of similarity techniques to calculations of the amplifier efficiency with varying undulator parameters. We give the first description of a scheme for an engineering calculation of the optimal undulator parameters and output characteristics of a FEL amplifier with optimal undulator.

In all the equations we use the Gaussian system of electromagnetic units, and the time dependence is taken to be of the form $\exp(-i\omega t)$.

1. THE LINEAR AMPLIFICATION REGIME

Preliminary remarks

We shall consider the linear operating regime of a FEL amplifier with the following assumptions: (1) the electron beam has a uniform density distribution in the direction perpendicular to the undulator axis; (2) the electrons move along identical trajectories parallel to the undulator axis; and (3) the amplified wave is a plane wave.

Many studies by various authors have been devoted to the problem discussed in this section. Those of Refs. 1–3 are important. The authors of Ref. 1 carried out the first theoretical study of the linear operating regime of a FEL amplifier using the above approximations. They obtained the self-consistent field equations and derived from them a characteristic equation taking into account the effects of the space charge and the energy spread of the beam particles. In Ref. 2 the Laplace-transform method was used to obtain the solution of the initial-value problem for the simplest case where the energy-spread effect is absent. The most complete analysis of the solutions of the initial-value problem using the Laplace-transform method is that of Ref. 3. The authors of that study obtained the Laplace transform of the self-consistent field equations, taking into account the effect of the energy spread of the beam particles, and managed to derive from them an expression for the Laplace transform of the field amplitude. The desired amplitude itself can be found by means of the inverse transform. This requires the computation of a complicated integral. For a number of cases, for example, for a Lorentzian energy spread, this integral can be transformed to an integral along a closed contour in the complex plane and calculated using residue theory. This mathematical trick does not work for a Gaussian energy distribution, and in that case the authors[3] solved the initial-value problem using numerical methods. However, it is important to note that in practice there is often no need for a complete solution of the initial-value problem, since it is sufficient to consider only the case of high gain. The present study is the first to point out the fact that in the limit of high gain the Laplace-transform method can be used to obtain an analytic solution of the initial-value problem even in the case of a Gaussian energy spread. The corresponding asymptotic expression for the gain is derived in this section.

The effective Hamiltonian

Let us consider a FEL amplifier with a helical undulator, the magnetic field of which varies according to the law

$$\mathbf{H}_0(z)=\mathbf{e}_x H_0\cos(\kappa_0 z)-\mathbf{e}_y H_0\sin(\kappa_0 z).$$

Here $\mathbf{e}_{x,y}$ are unit vectors directed along the x and y axes of a Cartesian coordinate system (x,y,z). It is assumed that the beam electrons are displaced only along the z axis in the undulator. The rotation angle θ_0 of the electrons in the undulator is assumed to be small, and the longitudinal component of the electron velocity v_z is taken to be close to the speed of light, $v_z \cong c$.

We represent the electric field vector of a circularly polarized electromagnetic wave moving along the undulator axis (the z axis) in complex form:

$$E_x + iE_y = \tilde{E}(z)\exp[i\omega(z/c - t)].$$

The complex amplitude of the field $\tilde{E}$ at any point in space is independent of the time t. This corresponds to the usual formulation of the problem with certain conditions at the undulator input at $z=0$. The frequency ω is a real quantity and corresponds to the frequency of the signal entering the amplifier input. We also assume that the complex amplitude of the field of the amplified wave $\tilde{E}$ is a slowly varying function of the coordinate z in the sense that $|\partial\tilde{E}/\partial z| \ll \kappa_0|\tilde{E}|$.

Let us consider the Hamiltonian formalism for the equations of motion of the beam electrons in the total electromagnetic field of the undulator, the radiation, and the space charge. The Hamiltonian is defined as

$$\mathscr{H}(p_z,z,t) = [(p_z c - eA_z)^2 + e^2(\mathbf{A}_\perp + A_0)^2 + m_0^2c^4]^{1/2} + e\varphi.$$

Here e is the electron charge, m_0 is the electron rest mass, p_z is the longitudinal component of the generalized particle momentum, $A_\perp$ is the vector potential of the wave, φ and A_z are respectively the scalar potential and vector potential of the space-charge field, and

$$\mathbf{A}_0(z) = -\mathbf{e}_z \times \int \mathbf{H}_0(z)dz$$

is the vector potential of the undulator field. In the one-dimensional model the transverse generalized momentum of the particle is an integral of the motion, and we take it to be zero. We transform the Hamiltonian $\mathscr{H}$ from the variables p_z, z, and t to variables convenient for describing the amplification process. We choose z as the new time coordinate, and we take the phase $\psi = \kappa_0 z + \omega(z/c - t)$ as the new generalized coordinate. We shall treat the transformation to these new variables as a canonical transformation. In our case the condition for a transformation to be canonical is conveniently written as equality of the action variation in the old and new coordinates:

$$-\mathscr{H}\delta t + p_z\delta z = -\tilde{\mathscr{H}}\delta z + \mathscr{P}\delta\psi, \qquad (1)$$

where $\tilde{\mathscr{H}}$ is the new Hamiltonian and $\mathscr{P}$ is the new generalized momentum, which is canonically conjugate to the phase ψ. We express the time variation δt as the variation of the new coordinate $\delta\psi$ and the new time δz:

$$-\delta t = \delta\psi/\omega - (\kappa_0 + \omega/c)\delta z/\omega. \qquad (2)$$

Substituting (2) into (1) and equating the coefficients of identical variations, we obtain $\mathscr{P} = \mathscr{H}/\omega$. The equations of motion preserve their canonical form with the new Hamiltonian:

$$\tilde{\mathscr{H}}(\mathscr{E},\psi,z) = (\kappa_0 + \omega/c)\mathscr{H}/\omega - p_z = (\kappa_0 + \omega/c)\mathscr{H}/\omega - eA_z/c - c^{-1}[(\mathscr{H} - e\varphi)^2 - e^2(A_\perp + A_0)^2 - m_0^2c^4]^{1/2}. \qquad (3)$$

For our purposes it is convenient to transform this Hamiltonian to another equivalent form. It follows from the Maxwell equations that the scalar potential φ and the longitudinal component of the vector potential A_z can be subjected to a gauge transformation

$$\varphi \to \varphi' = \varphi - c^{-1}\partial\chi/\partial t, \quad A_z \to A_z' = A_z + \partial\chi/\partial z,$$

where χ is an arbitrary function of the coordinate z and the time t. Here the longitudinal component of the electric field

$$E_z = -\partial\varphi/\partial z - c^{-1}\partial A_z/\partial t$$

remains invariant. We note that the generalized momentum $\mathscr{P}$ is not gauge-invariant, but is defined with the same arbitrariness as the potentials. We make a gauge transformation with the function

$$\chi = c\int dt\varphi(z,t).$$

This transformation eliminates the scalar potential, and the field is described by only the vector potential. As a result, the Hamiltonian (3) takes the form

$$\tilde{\mathscr{H}} = (\kappa_0 + \omega/c)\mathscr{E}/\omega - c^{-1}[\mathscr{E}^2 - e^2(\mathbf{A}_\perp + A_0)^2 - m_0^2c^4]^{1/2} - \frac{e}{\omega}\int d\psi E_z(z,\psi).$$

Now the interaction of the electron with the space-charge field is expressed entirely in terms of the longitudinal electric field E_z. In the gauge that we have used the generalized momentum $\mathscr{P}$ is the particle kinetic energy $\mathscr{E}$ divided by the frequency ω.

Before turning to the calculations of the interactions between the electrons and the wave in the undulator, the Hamiltonian that we have obtained can be simplified in two stages. First, $\tilde{\mathscr{H}}$ can be expanded in powers of the vector potential of the wave field $A_\perp$, keeping only the first-order terms. This approximation is valid when the transverse motion of the particles is determined by the undulator field rather than the wave field, i.e., when the condition

$$E_\perp(1 - v_z/c) \ll H_0$$

is satisfied. Here $E_\perp = c^{-1}|\partial A_\perp/\partial t|$ is the amplitude of the electric field of the wave. In the first order of the expansion in $A_\perp$ the Hamiltonian is

$$\tilde{\mathscr{H}} = (\mathscr{E}/\omega)(\kappa_0 + \omega/c) - c^{-1}[\mathscr{E}^2 - e^2|\mathbf{A}_0|^2 - m_0^2c^4]^{1/2} + (e^2/c)\mathbf{A}_\perp\cdot\mathbf{A}_0[\mathscr{E}^2 - e^2|\mathbf{A}_0|^2 - m_0^2c^4]^{-1/2} - \frac{e}{\omega}\int d\psi E_z. \qquad (4)$$

The second stage is to expand the Hamiltonian in small deviations of the particle energy from the value $\mathscr{E} = \mathscr{E}_0$, keeping only second-order terms. The final expression for the effective Hamiltonian is

$$H(P,\psi,z)=CP+\frac{\omega}{2c\gamma_z^2\mathscr{E}_0}P^2-(Ue^{i\psi}+U^*e^{-i\psi})$$

$$-\int d\psi eE_z, \qquad (5)$$

where $P=\mathscr{E}-\mathscr{E}_0$; $C=\kappa_0-\omega/(2c\gamma_z^2)$ is the detuning from resonance of a particle of energy $\mathscr{E}=\mathscr{E}_0$; $U=-e\theta_0\tilde{E}(z)/(2i)$ is the complex amplitude of the effective interaction potential; $\theta_0=eH_0/(\mathscr{E}_0\kappa_0)$; $\gamma_z^{-2}=\gamma^{-2}+\theta_0^2$; and $\gamma=\mathscr{E}_0/(m_0c^2)$.

The self-consistent field equations

The equation for the electron distribution function $f(P,\psi,z)$ is

$$\frac{\partial f}{\partial z}+\frac{\partial H}{\partial P}\frac{\partial f}{\partial \psi}-\frac{\partial H}{\partial \psi}\frac{\partial f}{\partial P}=0. \qquad (6)$$

We shall seek solutions for f and E_z in the linear approximation in the form

$$f=f_0+f_1e^{i\psi}+f_1^*e^{-i\psi},\quad E_z=\tilde{E}_ze^{i\psi}+\tilde{E}_z^*e^{-i\psi}. \qquad (7)$$

Since the problem is one-dimensional, from the Maxwell equations we have the following equation for E_z:

$$\partial E_z/\partial t=-4\pi j_z=-4\pi j_1\cos(\psi+\psi_1).$$

Here j_1 and ψ_1 are, respectively, the amplitude and phase of the first harmonic of the beam density, which are related to the complex amplitudes $\tilde{j}_1(z)$ and $f_1(P,z)$ as

$$\frac{1}{2}j_1\exp(i\psi_1)=\tilde{j}_1=\int f_1dP.$$

Then, using (7), we find the following expression for the amplitude $\tilde{E}_z$:

$$\tilde{E}_z=-i4\pi\tilde{j}_1(z)/\omega. \qquad (8)$$

The evolution of the amplitude f_1 according to Eqs. (5)–(8) is described by the equation

$$\frac{\partial}{\partial z}f_1+i(C+\omega P/(c\gamma_z^2\mathscr{E}_0))f_1+i(U$$

$$-4\pi e\tilde{j}_1(z)/\omega)\frac{\partial}{\partial P}f_0=0. \qquad (9)$$

In (9) we have omitted the term proportional to $\partial U/\partial P$. It can be shown that the effect of this term on the evolution of f_1 is negligible for our restrictions on the beam and undulator parameters. This point is discussed in more detail in Sec. 2. For definiteness, we shall consider the case where the beam is not modulated either in velocity or in density at the undulator input, i.e.,

$$f_1|_{z=0}=0,\quad f_0|_{z=0}=j_0F(P), \qquad (10)$$

where in our notation j_0 is equal to the average density of the beam current. The distribution function $F(P)$ is normalized by the condition

$$\int F(P)dP=1.$$

The solution of (9) taking into account (10) has the form

$$\tilde{j}_1(z)=j_0\int_0^z dz'\{e\theta_0\tilde{E}(z')/2$$

$$-4\pi ie\tilde{j}_1(z')/\omega\}\int dP(dF(P)/dP)$$

$$\times\exp\{i[C+\omega P/(c\gamma_z^2\mathscr{E}_0)](z'-z)\}. \qquad (11)$$

Another relation between the amplitudes $\tilde{j}_1(z)$ and $\tilde{E}(z)$ must come from the solution of the electrodynamical problem. The vector potential of the radiation field can be found using the wave equation

$$\nabla^2\mathbf{A}_\perp-c^{-2}\partial^2\mathbf{A}_\perp/\partial t^2=-(4\pi/c)\mathbf{j}_\perp,$$

where the density of the transverse current in the case under consideration has the form

$$j_x+ij_y=j_1\theta_0\exp(-i\kappa_0z)\cos(\psi+\psi_1).$$

We shall seek a solution for $A_\perp(z,t)$ in the form

$$A_{x,y}=\tilde{A}_{x,y}(z)\exp[i\omega(z/c-t)]+\text{C.C.},$$

in which we have explicitly isolated the strong z dependence of $A_\perp$. From the wave equation we have

$$\exp[i\omega(z/c-t)]\left\{2i\frac{\omega}{c}\frac{\partial}{\partial z}\begin{pmatrix}\tilde{A}_x\\ \tilde{A}_y\end{pmatrix}+\frac{\partial^2}{\partial z^2}\begin{pmatrix}\tilde{A}_x\\ \tilde{A}_y\end{pmatrix}\right\}+\text{C.C.}$$

$$=-4\pi\theta_0c^{-1}\begin{pmatrix}\cos(\kappa_0z)\\ -\sin(\kappa_0z)\end{pmatrix}j_1\cos(\psi+\psi_1). \qquad (12)$$

If in (12) we neglect rapidly oscillating terms of the type

$$\exp\{\pm i[2\kappa_0z+\omega(z/c-t)]\},$$

then Eq. (12) can be transformed to an equation containing only slowly varying amplitudes:

$$d\tilde{E}/dz=-\pi\theta_0c^{-1}\tilde{j}_1(z). \qquad (13)$$

Here we have used the fact that the vector potential and the electrical field vector of the electromagnetic wave in our one-dimensional approximation are related as $E_{x,y}=-\partial(A_{x,y})/\partial t$. The characteristic scale of variation of the complex amplitude $\tilde{E}$ is much larger than the wavelength, so in (13) we have omitted the second derivative of $\tilde{E}$ with respect to z. Substituting (11) into the right-hand side of (13), we easily obtain a single integro-differential equation for the desired amplitude $\tilde{E}$. For the rest of our discussion it is convenient to transform to dimensionless variables, which are introduced by the relations $\hat{z}=\Lambda_0z$, $\hat{C}=C/\Lambda_0$, $\hat{P}=\omega P/(c\gamma_z^2\mathscr{E}_0\Lambda_0)$, and $\hat{\kappa}_p^2=\kappa_p^2/\Lambda_0^2$. Here $\Lambda_0=[\pi j_0\theta_0^2c^{-1}\omega\gamma_z^{-2}\gamma^{-1}I_A^{-1}]^{1/3}$ is the amplification factor; $\kappa_p=[4\pi_0j_0\gamma_z^{-2}\gamma^{-1}I_A^{-1}]^{1/2}$ is the longitudinal plasma wave number; and $I_A\cong17$ kA is the Alfvén current. As a result, we obtain the following dimensionless working equation:

$$\frac{\partial\tilde{E}}{\partial\hat{z}}=\int_0^{\hat{z}}d\hat{z}'\left\{\tilde{E}(\hat{z}')+i\hat{\kappa}_p^2\frac{\partial\tilde{E}(\hat{z}')}{d\hat{z}'}\right\}\int_{-\infty}^{\infty}d\hat{P}\frac{d\hat{F}}{d\hat{P}}$$

$$\times\exp\{i(\hat{P}+\hat{C})(\hat{z}'-\hat{z})\}. \qquad (14)$$

Here $\hat{F}(\hat{P})$ is the distribution in the normalized momentum $\hat{P}$ satisfying the normalization condition $\int \hat{F}(\hat{P})d\hat{P}=1$.

Solution of the self-consistent field equations by the Laplace method

Equation (14) is an integro-differential equation for the field amplitude $\tilde{E}(\hat{z})$ and can be solved by a Laplace transform. It is well known that such a transform is defined by the integral ($\mathrm{Re}p>0$)

$$\overline{E}(p)=\int_0^\infty d\zeta \exp(-p\zeta)\tilde{E}(\zeta).$$

The Laplace transform of Eq. (14) has the form

$$p\overline{E}(p)-E_{\mathrm{ext}}=[\overline{E}(p)+\mathrm{i}\hat{\kappa}_p^2(p\overline{E}(p)-E_{\mathrm{ext}})]\times\int_{-\infty}^{\infty}d\xi\frac{F'(\xi)}{p+\mathrm{i}(\xi+\hat{C})}. \tag{15}$$

Here E_{ext} is the amplitude of the wave field at the undulator input at $z=0$. If we solve Eq. (15) for $\overline{E}(p)$, we obtain the expression

$$\overline{E}(p)=\frac{E_{\mathrm{ext}}}{p-\hat{D}/(1-\mathrm{i}\hat{\kappa}_p^2\hat{D})}. \tag{16}$$

Here we have introduced the notation

$$\hat{D}=\int_{-\infty}^{\infty}d\xi\frac{\hat{F}'(\xi)}{p+\mathrm{i}(\xi+\hat{C})}. \tag{17}$$

In order to find $\tilde{E}(\hat{z})$ we must take the inverse Laplace transform of (16). This transform is defined by the integral

$$\tilde{E}(\hat{z})=\frac{1}{2\pi\mathrm{i}}\int_{\gamma'-\mathrm{i}\infty}^{\gamma'+\mathrm{i}\infty}d\lambda\overline{E}(\lambda)\exp(\lambda\hat{z})$$

$$=\frac{E_{\mathrm{ext}}}{2\pi\mathrm{i}}\int_{\gamma'-\mathrm{i}\infty}^{\gamma'+\mathrm{i}\infty}d\lambda\frac{\exp(\lambda\hat{z})}{\lambda-\hat{D}/(1-\mathrm{i}\hat{\kappa}_p^2\hat{D})}. \tag{18}$$

Let the integration in the complex λ plane run parallel to the imaginary axis. The constant γ' is a real positive number, larger than the real parts of all the singularities of the integrand. The linear integral (18) obtained by the inverse transform is usually calculated by closing the integration contour by a semicircle at infinity in the left half-plane and using the residue theorem. For this trick to be applicable to the integral (18) it is necessary that the integrand in (18) have an analytic continuation into the left half-plane, and that the coefficient of $\exp(\lambda\hat{z})$ in the integrand in (18) satisfy the conditions of Jordan's lemma.

According to (17), the function $\hat{D}$ is a complex integral and has a discontinuity on the imaginary λ axis. This integral becomes an analytic function if, following Landau's method,[4] the function $\hat{D}$ is defined as

$$\hat{D}=\int_{-\infty}^{\infty}d\xi\frac{\hat{F}'(\xi)}{\lambda+\mathrm{i}(\xi+\hat{C})},\quad \mathrm{Re}\,\lambda>0;$$

$$\hat{D}=P\int_{-\infty}^{\infty}d\xi\frac{\hat{F}'(\xi)}{\lambda+\mathrm{i}(\xi+\hat{C})}+\pi\hat{F}'(\mathrm{i}\lambda-\hat{C}),\quad \mathrm{Re}\,\lambda=0;$$

$$\hat{D}=\int_{-\infty}^{\infty}d\xi\frac{\hat{F}'(\xi)}{\lambda+\mathrm{i}(\xi+\hat{C})}+2\pi\hat{F}'(\mathrm{i}\lambda-\hat{C}),\quad \mathrm{Re}\,\lambda<0. \tag{19}$$

Here $P(...)$ denotes the principal value. If the distribution function $\hat{F}(\hat{P})$ is such that the coefficient

$$\frac{1}{\lambda-\hat{D}/(1-\mathrm{i}\hat{\kappa}_p^2\hat{D})}$$

of $\exp(\lambda\hat{z})$ in the integrand in (18) satisfies the conditions of Jordan's lemma, the complete wave field can be represented as a superposition of partial waves. Finally, using the residue theorem, we obtain the following expression for $\tilde{E}(\hat{z})$:

$$\tilde{E}(z)=E_{\mathrm{ext}}\sum_j\frac{\exp(\lambda_j\hat{z})}{1-\hat{D}_j'/(1-\mathrm{i}\hat{\kappa}_p^2\hat{D})^2}. \tag{20}$$

Here we have introduced the abbreviated notation

$$\hat{D}_j=\hat{D}|_{\lambda=\lambda_j},\quad \hat{D}_j'=\left.\frac{d\hat{D}}{d\lambda}\right|_{\lambda=\lambda_j},$$

where λ_j is the jth root of the equation

$$\lambda-\hat{D}/(1-\mathrm{i}\hat{\kappa}_p^2\hat{D})=0, \tag{21}$$

and the function $\hat{D}$ is defined by Eq. (19).

Solution of the initial-value problem for the case of a cold electron beam

As an illustration of the use of the expressions we have obtained, let us consider the case of small energy spread, when the distribution function $\hat{F}(\hat{P})$ can be replaced by a delta function $\hat{F}(\hat{P})=\delta(\hat{P})$. In this case the function $\hat{D}$ is given in the entire complex λ plane by

$$\hat{D}=\mathrm{i}(\lambda+\mathrm{i}\hat{C})^{-2}.$$

Since the coefficient of $\exp(\lambda\hat{z})$ in (18),

$$\frac{1}{\lambda-\hat{D}/(1-\mathrm{i}\hat{\kappa}_p^2\hat{D})}=\frac{1}{\lambda-\mathrm{i}/[(\lambda+\mathrm{i}\hat{C})^2+\hat{\kappa}_p^2]},$$

is of order λ^{-1} for $|\lambda|\Rightarrow\infty$, the condition of Jordan's lemma is satisfied. Therefore, Eq. (20) is applicable and the partial-wave expansion of the wave has the form

$$\tilde{E}(\hat{z})=E_{\mathrm{ext}}\sum_j\frac{\exp(\lambda_j\hat{z})}{1-2\mathrm{i}(\lambda_j+\mathrm{i}\hat{C})\lambda_j^2},$$

where λ_j are the roots of the cubic equation

$$\lambda=\mathrm{i}[(\lambda+\mathrm{i}\hat{C})^2+\hat{\kappa}_p^2]^{-1}. \tag{22}$$

Using the relations between the roots of the cubic equation (22),

$$\lambda_1\lambda_2\lambda_3=i,\quad \lambda_1\lambda_2+\lambda_2\lambda_3+\lambda_1\lambda_3=-\hat{C}^2+\hat{\kappa}_p^2,$$

$$\lambda_1+\lambda_2+\lambda_3=-2\mathrm{i}\hat{C},$$

after simple algebra we obtain the familiar expression for the wave amplitude:[2,3]

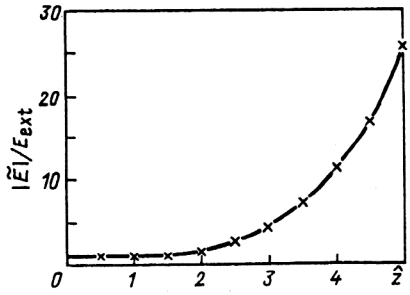

FIG. 1. The linear regime. Dependence of the amplitude of the wave field, normalized to the amplitude of the input signal, on the normalized length for $\hat{C}=0$, $\hat{\kappa}_p^2=0$, and $\hat{\Lambda}_T^2=0$. The solid line was calculated using the analytic expression (24), and the crosses are the results of numerical modeling using Eqs. (44) and (45).

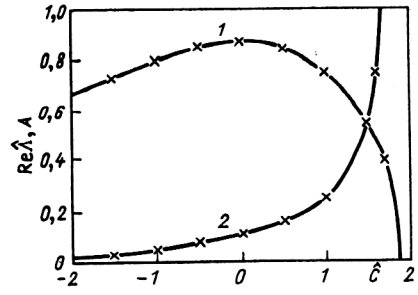

FIG. 2. The linear regime. Dependence on the normalized detuning $\hat{C}$ for $\hat{\kappa}_p^2=0$, $\hat{\Lambda}_T^2=0$. Curve 1 is the normalized increment from Eq. (26), curve 2 is the pre-exponential factor from Eq. (27), and the crosses are the result of numerical modeling using Eqs. (44) and (45).

$$\tilde{E}(\hat{z})=E_{ext}\left\{\frac{\lambda_2\lambda_3\exp(\lambda_1\hat{z})}{(\lambda_1-\lambda_2)(\lambda_1-\lambda_3)}+\frac{\lambda_1\lambda_3\exp\lambda_2(\hat{z})}{(\lambda_2-\lambda_3)(\lambda_2-\lambda_1)}\right.$$
$$\left.+\frac{\lambda_1\lambda_2\exp(\lambda_3\hat{z})}{(\lambda_3-\lambda_1)(\lambda_3-\lambda_2)}\right\}, \tag{23}$$

Exactly on resonance ($\hat{C}=0$) in the absence of the space-charge and energy-spread effects the solution for $\hat{E}(z)$ is written as

$$\tilde{E}(z)=\frac{1}{3}E_{ext}\left\{\exp\left(\frac{\sqrt{3}+i}{2}\hat{z}\right)+\exp\left(\frac{-\sqrt{3}+i}{2}\hat{z}\right)\right.$$
$$\left.+\exp(-i\hat{z})\right\}. \tag{24}$$

The graph of the dependence of $|\tilde{E}|/E_{ext}$ on the dimensionless length $\hat{z}$ in the initial section of the undulator calculated using Eq. (24) is shown in Fig. 1. If the undulator length is sufficiently large, the contribution in (24) from the growing wave will exceed the other terms, and their contribution can be neglected. Then for $\tilde{E}(\hat{z})$ we can write the asymptotic expression

$$\tilde{E}(\hat{z})=\frac{1}{3}E_{ext}\exp\left(\frac{\sqrt{3}+i}{2}\hat{z}\right). \tag{25}$$

An important output characteristic of the amplifier is the power gain $G=|\tilde{E}|^2/E_{ext}^2$. According to (25), the value of G' in decibels for $\hat{C}=0$ is asymptotically equal to

$$G=10\lg(|\tilde{E}|^2/E_{ext}^2)=7.5\hat{z}-9.5.$$

It follows from Eq. (22) that for $\hat{\kappa}_p^2=0$ the partial-wave propagation constants λ_1, λ_2, and λ_3 are universal functions of only the detuning parameter $\hat{C}$. Study of the characteristic equation

$$\lambda(\lambda+i\hat{C})^2=i \tag{26}$$

shows that one of the partial waves is a growing wave in the detuning range $\hat{C}<1.89$. We denote the propagation constant of the growing partial wave by $\hat{\Lambda}$. Then in the detuning range $\hat{C}<1.89$ the power gain for a sufficiently long undulator can be written asymptotically as

$$G=A\exp[2\,\mathrm{Re}(\hat{\Lambda})\hat{z}], \tag{27}$$

where the increment $\mathrm{Re}(\hat{\Lambda})$ and the pre-exponential factor A are universal functions of the detuning parameter $\hat{C}$. Graphs of these functions are shown in Fig. 2. The maximum increment is reached exactly at resonance ($\hat{C}=0$). For small deviations from resonance, when $\hat{C}\ll 1$, the increment is given by

$$2\,\mathrm{Re}(\hat{\Lambda})=\sqrt{3}[1-\hat{C}^2/9].$$

For large negative detunings $\hat{C}\ll -1$ we asymptotically have

$$\mathrm{Re}(\hat{\Lambda})=|\hat{C}|^{-1/2}.$$

The electromagnetic-wave amplification process in an undulator displays resonance behavior, which causes the amplification factor to depend strongly on the detuning parameter $\hat{C}$. Usually the amplification bandwidth is defined as the difference of the input signal frequencies $\omega_1-\omega_2=\Delta\omega$ for which the power output is decreased by a factor of 2 relative to its maximum. It is convenient to introduce the amplification bandwidth in the reduced detuning $\Delta\hat{C}$, which is related to the amplification bandwidth in the frequency of the input signal as $\Delta\omega/\omega_0=(\Lambda_0/\kappa_0)\Delta\hat{C}$, where $\omega_0=2c\gamma_z^2\kappa_0$ is the resonance frequency. The amplification bandwidth can be found by solving the initial-value problem. In Fig. 3 we show a graph of the dependence of the amplification bandwidth $\Delta\hat{C}$ on the maximum power gain. This graph was calculated using Eq. (23) and the roots of the characteristic equation (26). As an illustration, in Fig. 4 we give a graph of the amplitude–frequency characteristic for the maximum gain $G_{max}=40$ dB.

Let us now consider the effect of the space-charge field on the wave amplification process in the undulator. In the region of parameters of the problem where the space-charge parameter $\hat{\kappa}_p^2$ is small, the space-charge effect can be included using perturbation theory. After simple calculations using Eq. (22), we find that for $\hat{\kappa}_p^2\ll 1$ the maximum increment is attained for the detuning parameter $\hat{C}=\hat{C}_m=\hat{\kappa}_p^2$ and is given by

$$\max[2\,\mathrm{Re}(\hat{\Lambda})]=3^{1/2}-3^{-1/2}\hat{\kappa}_p^2.$$

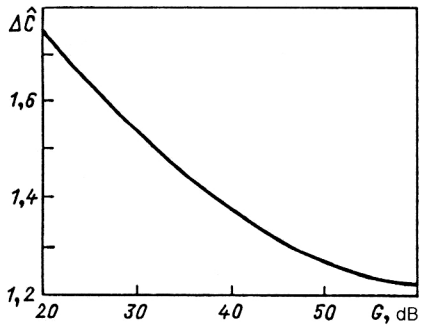

FIG. 3. The linear regime. Dependence of the normalized amplification bandwidth on the maximum power gain for $\hat{C}=0$, $\hat{\kappa}_p^2=0$, and $\hat{\Lambda}_T^2=0$.

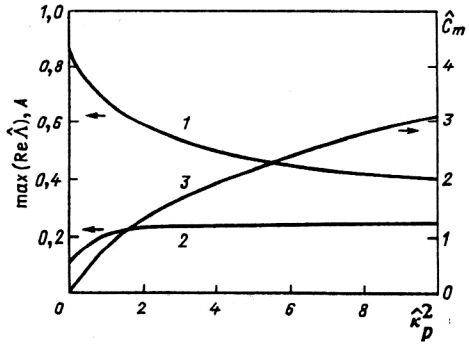

FIG. 5. The linear regime. Results of calculations using Eqs. (22), (23), and (27) for tuning to the maximum increment. Dependence of the maximum of the normalized increment (curve 1), the pre-exponential factor from (27) (curve 2), and the optimal normalized detuning (curve 3) on the space-charge parameter $\hat{\kappa}_p^2$ for $\hat{\Lambda}_T^2=0$.

In the opposite case $\hat{\kappa}_p^2 \gg 1$ the space-charge field significantly affects the increment, which at the maximum for $\hat{C}=\hat{C}_m=\hat{\kappa}_p$ is equal to[1]

$$\max[2\,\mathrm{Re}(\hat{\Lambda})]=(2\hat{\kappa}_p)^{-1/2}.$$

In the region where the space-charge parameter is comparable to unity, the increment can be found by solving the cubic characteristic equation (22). It should be noted that, according to Eq. (22), the maximum increment and the detuning $\hat{C}_m$ for which this maximum is reached are universal functions of the space-charge parameter κ_p^2. The pre-exponential factor A in the asymptotic expression for the amplification (27) for tuning to the maximum increment (i.e., for $\hat{C}=\hat{C}_m$) is also a universal function of the parameter κ_p^2. Graphs of these functions are shown in Fig. 5. As an illustration, in Fig. 6 we show the curve describing the dependence of the increment on the detuning for $\hat{\kappa}_p^2=1$.

In the calculations carried out above it was assumed that an unmodulated electron beam and the electromagnetic wave from a master oscillator are fed to the amplifier input. This is discussed in more detail in Appendix A.

Solution of the initial-value problem for the case of a Lorentzian energy spread

Let us consider the case of an electron beam whose energy distribution function is given by a Lorentzian distribution

$$F(\mathscr{E})=(\alpha/\pi)[(\mathscr{E}-\mathscr{E}_0)^2+\alpha^2]^{-1}.$$

The expression for the dimensionless quantity $\hat{F}$ will have the form

$$\hat{F}(\hat{P})=(\hat{\alpha}/\pi)[\hat{P}^2+\hat{\alpha}^2]^{-1}. \tag{28}$$

The relation between the parameters α and $\hat{\alpha}$ is given by

$$\hat{\alpha}=\alpha\omega/(\gamma_z^2 c\mathscr{E}_0\Lambda_0).$$

Substituting (28) into (19), we find that in the case of a Lorentzian distribution, the function $\hat{D}$ in the entire complex λ plane is given by

$$\hat{D}=\mathrm{i}(\lambda+\hat{\alpha}+\mathrm{i}\hat{C})^{-2}.$$

The coefficient of $\exp(\lambda\hat{z})$ in the integrand in (18) in this case is equal to

$$\left\{\lambda-\frac{\hat{D}}{1-\mathrm{i}\hat{\kappa}_p^2\hat{D}}\right\}^{-1}=\left\{\lambda-\frac{\mathrm{i}}{[(\lambda+\hat{\alpha}+\mathrm{i}\hat{C})^2+\hat{\kappa}_p^2]}\right\}^{-1}$$

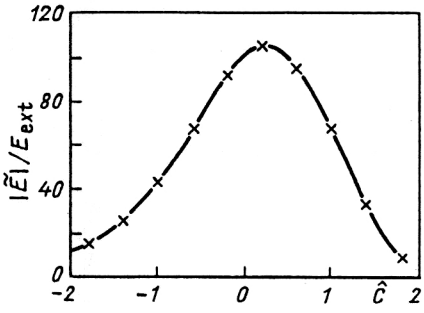

FIG. 4. The linear regime. Dependence of the field amplitude at the amplifier output, normalized to the amplitude of the input signal, on the normalized detuning. The normalized length of the amplifier is $\hat{z}=6.6$, $\hat{\kappa}_p^2=0$, and $\hat{\Lambda}_T^2=0$.

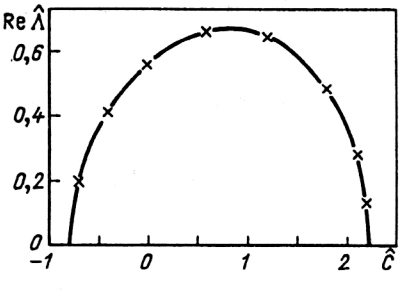

FIG. 6. The linear regime. Dependence of the normalized increment on the normalized detuning for $\hat{\kappa}_p^2=1$ and $\hat{\Lambda}_T^2=0$. The solid line is the result of solving Eq. (22), and the crosses are the result of numerical modeling using Eqs. (45) and (52).

and obviously satisfies the conditions of Jordan's lemma. Therefore, Eq. (20) is applicable:

$$\tilde{E}(\hat{z})=E_{\text{ext}}\sum_j \frac{\exp(\lambda_j\hat{z})}{1-2i(\lambda_j+\hat{\alpha}+i\hat{C})\lambda_j^2}.$$

Here λ_j are the roots of the cubic equation

$$\lambda=i[(\lambda+\hat{\alpha}+i\hat{C})^2+\hat{\kappa}_p^2]^{-1}.$$

Therefore, in the case of a Lorentzian distribution the electromagnetic wave in the undulator can be represented as the sum of three partial waves.

Solution of the initial-value problem for the case of a Gaussian energy distribution

We conclude this section by considering the case of a Gaussian energy distribution:

$$F(\mathscr{E}-\mathscr{E}_0)=[2\pi\langle(\Delta\mathscr{E})^2\rangle]^{-1/2}\times\exp\left[-\frac{(\mathscr{E}-\mathscr{E}_0)^2}{2\langle(\Delta\mathscr{E})\rangle^2}\right].$$

The corresponding distribution in the normalized canonical momentum $\hat{P}$ has the form

$$\hat{F}(\hat{P})=(4\pi\hat{\Lambda}_T^2)^{-1/2}\exp[-\hat{P}^2/(4\hat{\Lambda}_T^2)].$$

The parameter $\hat{\Lambda}_T^2$ is related to the rms energy spread $\langle(\Delta\mathscr{E})^2\rangle$ as

$$\hat{\Lambda}_T^2=\omega^2\langle(\Delta\mathscr{E})^2\rangle/(2\gamma_z^4c^2\Lambda_0^2\mathscr{E}_0^2).$$

We begin the calculation of the function $\hat{D}$ with the case $\mathrm{Re}\lambda>0$. From Eq. (19) we have

$$\hat{D}=\int_{-\infty}^{\infty}d\xi\frac{\hat{F}'(\xi)}{\lambda+i(\xi+\hat{C})}=i\int_{-\infty}^{\infty}d\xi\frac{\hat{F}(\xi)}{[\lambda+i(\xi+\hat{C})]^2},\quad \mathrm{Re}\,\lambda>0. \tag{29}$$

Substituting the equation

$$\frac{1}{[\lambda+i(\xi+\hat{C})]^2}=\int_0^{\infty}\tau\exp\{-[\lambda+i(\xi+\hat{C})]\tau\}d\tau$$

into (29) and integrating over ξ first, we obtain

$$\hat{D}=i\int_0^{\infty}\tau\exp\{-\hat{\Lambda}_T^2\tau^2-[\lambda+i\hat{C}]\tau\}d\tau,\quad \mathrm{Re}\,\lambda>0. \tag{30}$$

In the left half-plane, using Eq. (19) and the expression

$$\frac{1}{[\lambda+i(\xi+\hat{C})]^2}=\int_0^{\infty}\tau\exp\{[\lambda+i(\xi+\hat{C})]\tau\}d\tau,\quad \mathrm{Re}\,\lambda<0,$$

the expression for the function $\hat{D}$ can be brought to the form

$$\hat{D}=i\int_0^{\infty}\tau\exp\{-\hat{\Lambda}_T^2\tau^2+[\lambda+i\hat{C}]\tau\}d\tau$$

$$-\frac{i}{2}\sqrt{\pi}l\hat{\Lambda}_T^{-3}[\lambda+i\hat{C}]\exp\left\{\frac{1}{4}\hat{\Lambda}_T^{-2}[\lambda+i\hat{C}]^2\right\},\quad \mathrm{Re}\,\lambda<0. \tag{31}$$

We note that the expression for $\hat{D}$ in the left half-plane contains a term proportional to $\exp(\lambda^2)$. Therefore, the function $\hat{D}$ has a singularity at infinity. In this case, as follows from the Picard theorem, the integrand in (18) has an infinite number of poles in the left half-plane, which bunch up at infinity and are located near the lines $\arg(\lambda)=\pm3\pi/4$. According to Jordan's lemma, the calculation of the linear integral (18) by closing the integration contour with an infinite semicircle in the left-hand plane is possible if the function $\bar{E}(\lambda)$ tends to zero for $|\lambda|\Rightarrow\infty$ uniformly in the argument of λ. This condition is not satisfied for the Gaussian distribution function. In this case the Laplace-transform method does not lead to an analytic solution of the initial-value problem in closed form. However, it is important to note that there is often no need of a complete solution to the initial-value problem, since it is sufficient to consider only the case of high gain. Below we show that for the Gaussian distribution function the Laplace-transform method can be used to obtain an asymptotic expression for the amplification of a FEL amplifier in closed form.

We shall use the following mathematical trick. Shifting the integration path in (18) to the left half-plane, we use the residue theorem to transform the linear integral to the form

$$\int_{\gamma'-i\infty}^{\gamma'+i\infty}d\lambda\bar{E}(\lambda)\exp(\lambda\hat{z})=\int_{-\alpha'-i\infty}^{-\alpha'+i\infty}d\lambda\bar{E}(\lambda)\exp(\lambda\hat{z})+\sum_{-\alpha'<\mathrm{Re}\,\lambda_j}\mathrm{Res}\,\bar{E}(\lambda_j)\exp(\lambda_j\hat{z}), \tag{32}$$

where the summation runs over the roots of Eq. (21) lying to the right of the line $(-\alpha'-i\infty,-\alpha'+i\infty)$. Here α' is a real positive number, and $\mathrm{Res}\bar{E}(\lambda_j)$ is the residue of the function $\bar{E}(\lambda)$ at the pole λ_j. Using Eqs. (30) and (31), it can easily be checked that there is only one root in the right half-plane of Eq. (21), and for any finite value of α' the number of roots in the interval $-\alpha'<\mathrm{Re}(\lambda)<0$ is always finite. If the undulator is sufficiently long, the contribution to (32) from the term proportional to $\exp(\lambda_1\hat{z})$ with $\mathrm{Re}(\lambda_1)>0$ will be greater than all the others, and the contribution of the latter can be neglected. Then for the amplitude $\tilde{E}(\hat{z})$ we can write down an asymptotic expression of the form

$$\tilde{E}(\hat{z})=E_{\text{ext}}\frac{\exp(\lambda_1\hat{z})}{1-\hat{D}_1'/(1-i\hat{\kappa}_p^2\hat{D}_1)^2}, \tag{33}$$

where the values of the functions $\hat{D}$ and $\hat{D}'$ at $\lambda=\lambda_1$ can be found from (30). The rest of the problem consists of casting Eq. (33) in a form convenient for numerical calculations.

We express the function $\hat{D}'(\lambda)$ in terms of the function $\hat{D}(\lambda)$. From integral tables we find the expression for $\mathrm{Re}(\lambda)>0$:

$$\hat{D}=\mathrm{i}\int_0^\infty \exp[-\hat{\Lambda}_\mathrm{T}^2\tau^2-(\lambda+\mathrm{i}\hat{C})\tau]\tau d\tau$$

$$=\frac{\mathrm{i}}{2\hat{\Lambda}_\mathrm{T}^2}-\frac{\mathrm{i}\sqrt{\pi}}{4\hat{\Lambda}_\mathrm{T}^3}(\lambda+\mathrm{i}\hat{C})\exp\left[\frac{1}{4\hat{\Lambda}_\mathrm{T}^2}(\lambda+\mathrm{i}\hat{C})^2\right]$$

$$\times\left\{1-\mathrm{erf}\left[\frac{1}{2\hat{\Lambda}_\mathrm{T}}(\lambda+\mathrm{i}\hat{C})\right]\right\};$$

$$\hat{D}'(\lambda)=-\mathrm{i}\int_0^\infty \exp[-\hat{\Lambda}_\mathrm{T}^2\tau^2-(\lambda+\mathrm{i}\hat{C})\tau]\tau^2 d\tau$$

$$=\frac{\mathrm{i}}{4\hat{\Lambda}_\mathrm{T}^4}(\lambda+\mathrm{i}\hat{C})-\frac{\mathrm{i}\sqrt{\pi}}{4\hat{\Lambda}_\mathrm{T}^5}\left[\frac{1}{2}(\lambda+\mathrm{i}\hat{C})^2+\hat{\Lambda}_\mathrm{T}^2\right]$$

$$\times\exp\left[\frac{1}{4\hat{\Lambda}_\mathrm{T}^2}(\lambda+\mathrm{i}\hat{C})^2\right]\left\{1-\mathrm{erf}\left[\frac{1}{2\hat{\Lambda}_\mathrm{T}}(\lambda+\mathrm{i}\hat{C})\right]\right\}.$$

Here $\mathrm{erf}(\zeta)$ denotes the error function of a complex argument:

$$\mathrm{erf}(\zeta)=2\pi^{-1/2}\int_0^\zeta \exp(-u^2)du.$$

In the end we obtain

$$\hat{D}'(\lambda)=\frac{\mathrm{i}}{4}\hat{\Lambda}_\mathrm{T}^{-4}[\lambda+\mathrm{i}\hat{C}]+\frac{1}{2}(\lambda+\mathrm{i}\hat{C})^2+\hat{\Lambda}_\mathrm{T}^2]$$

$$\times\hat{\Lambda}_\mathrm{T}^{-2}\left[\hat{D}-\frac{\mathrm{i}}{2}\hat{\Lambda}_\mathrm{T}^{-2}\right][\lambda+\mathrm{i}\hat{C}]^{-1}. \qquad (34)$$

Using Eq. (21), the value of the function $\hat{D}$ for $\lambda=\lambda_1$ can be expressed in terms of the root λ_1:

$$\hat{D}(\lambda_1)=\lambda_1[1+\mathrm{i}\hat{\kappa}_p^2\lambda_1]^{-1}. \qquad (35)$$

Using Eqs. (33)–(35), we easily obtain an asymptotic expression for the gain in a form convenient for numerical calculations:

$$\tilde{E}(\hat{z})=E_\mathrm{ext}\exp(\hat{\Lambda}z)\left\{1+\mathrm{i}(\mathrm{i}-\hat{\kappa}_p^2\hat{\Lambda})^2\right.$$

$$\times\left\{\left[\hat{\Lambda}(\mathrm{i}-\hat{\kappa}_p^2\hat{\Lambda})^{-1}-\frac{1}{2\hat{\Lambda}_\mathrm{T}^2}\right]\right.$$

$$\times\left[(\hat{\Lambda}+\mathrm{i}\hat{C})^{-1}+\frac{1}{2\hat{C}_\mathrm{T}^2}(\hat{\Lambda}+\mathrm{i}\hat{C})\right]$$

$$\left.\left.+\frac{1}{4\hat{\Lambda}_\mathrm{T}^4}(\hat{\Lambda}+\mathrm{i}C)\right\}\right\}^{-1}, \qquad (36)$$

where $\hat{\Lambda}=\lambda_1$ is the growing root of the characteristic equation

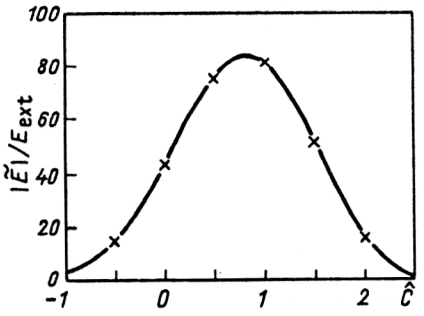

FIG. 7. The linear regime. Dependence of the field amplitude at the amplifier output, normalized to the amplitude of the input signal, on the normalized detuning for $\hat{\Lambda}_\mathrm{T}^2=0.1$, $\hat{\kappa}_p^2=0.5$, and $\hat{z}=8$. The solid line is the calculation using Eq. (36), and the crosses are the results of numerical modeling using Eqs. (45) and (52).

$$\hat{\Lambda}-\frac{\hat{D}}{1-\mathrm{i}\hat{\kappa}_p^2\hat{D}}=0,\quad \hat{D}=\mathrm{i}\int_0^\infty \exp[-\hat{\Lambda}_\mathrm{T}^2\tau^2-(\hat{\Lambda}+\mathrm{i}\hat{C})\tau]\tau d\tau,\quad \mathrm{Re}(\hat{\Lambda})>0.$$

A particularly simple expression is obtained when the space-charge effect is absent. In the limit $\hat{\kappa}_p^2\to 0$, from Eq. (36) we have

$$\tilde{E}(\hat{z})=2E_\mathrm{ext}\exp(\hat{\Lambda}\hat{z})\hat{\Lambda}_\mathrm{T}^2[\hat{\Lambda}+\mathrm{i}\hat{C}]$$

$$\times[2\mathrm{i}\hat{C}\hat{\Lambda}_\mathrm{T}^2+\mathrm{i}-\hat{\Lambda}(\hat{\Lambda}+\mathrm{i}C)^2]^{-1}, \qquad (37)$$

where $\hat{\Lambda}$ is the growing root of the characteristic equation

$$\hat{\Lambda}=\mathrm{i}\int_0^\infty \exp[-\hat{\Lambda}_\mathrm{T}^2\tau^2-(\hat{\Lambda}+\mathrm{i}\hat{C})\tau]\tau d\tau,\quad \mathrm{Re}(\hat{\Lambda})>0. \qquad (38)$$

An amplifier characteristic of practical importance is the power gain G, which for a sufficiently long undulator can be written as

$$G=|\tilde{E}|^2/E_\mathrm{ext}^2=A\exp[2\,\mathrm{Re}(\hat{\Lambda})\hat{z}], \qquad (39)$$

where in the general case A and $\hat{\Lambda}$ are functions of the parameters $\hat{C}$, $\hat{\kappa}_p^2$, and $\hat{\Lambda}_\mathrm{T}^2$. In Fig. 7 we show the dependence of the field amplitude at the amplitude output on $\hat{C}$ for $\hat{z}=8$. The space-charge and beam-spread parameters are for illustration taken to be $\hat{\kappa}_p^2=0.5$ and $\hat{\Lambda}_\mathrm{T}^2=0.1$. We constructed the curve using the results of the calculation carried out with the asymptotic amplification formula (36). For the parameter region where the space-charge effect can be neglected ($\hat{\kappa}_p^2\to 0$), the increment can be found by solving the transcendental characteristic equation (38). For a small energy spread, when $\hat{\Lambda}_\mathrm{T}^2\ll 1$, the maximum increment is attained for the detuning $\hat{C}=\hat{C}_m=6\hat{\Lambda}_\mathrm{T}^2$ and is

$$\max[2\,\mathrm{Re}(\hat{\Lambda})]=3^{1/2}-3^{1/2}2\hat{\Lambda}_\mathrm{T}^2.$$

In the opposite case, when $\hat{\Lambda}_\mathrm{T}^2\gg 1$, the energy spread significantly affects the increment, the maximum of which at $\hat{C}=2^{1/2}\hat{\Lambda}_\mathrm{T}$ is[1]

$$\max[\mathrm{Re}(\hat{\Lambda})]=0.38\hat{\Lambda}_\mathrm{T}^{-2}.$$

It should be noted that according to Eq. (38), the maximum of the increment and the detuning $\hat{C}_m$ at which this

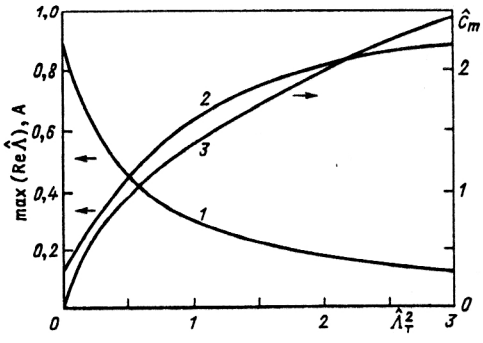

FIG. 8. The linear regime. Results of calculations using Eqs. (37)–(39) for tuning to the maximum increment. Dependence of the maximum of the normalized increment (curve 1), the pre-exponential factor (39) (curve 2), and the optimal normalized detuning (curve 3) on the energy-spread parameter $\hat{\Lambda}_T^2$ for $\hat{\kappa}_p^2 = 0$.

maximum is reached are universal functions of the energy-spread parameter $\hat{\Lambda}_T^2$. The pre-exponential factor A in the asymptotic amplification factor for tuning to the maximum increment (i.e., for $\hat{C} = \hat{C}_m$) is also a universal function of the parameter $\hat{\Lambda}_T^2$. Graphs of these functions are given in Fig. 8. For illustration, in Fig. 9 we show the curve describing the dependence of the increment on the detuning for the energy-spread parameter $\hat{\Lambda}_T^2 = 0.5$.

2. SATURATION EFFECTS

Preliminary remarks

In the preceding section we discussed computational methods applicable to the linear operating regime of a FEL amplifier. In this regime an increase of the input power W_{ext} leads to a directly proportional increase of the output power W_f. When W_{ext} is increased further, the operation of the amplifier becomes nonlinear. In the nonlinear regime W_f increases more slowly than W_{ext}, and at a certain value of W_{ext} the output power reaches a maximum. To determine the maximum W_f it is necessary to solve the equations of the nonlinear theory of the FEL amplifier. Analytical methods are of limited usefulness in the theoretical study of the nonlinear regime, and numerical modeling must be used. The first numerical calculations of the nonlinear operating regime of the FEL amplifier were carried out in Ref. 5, and they were developed further in the later studies of Refs. 6 and 7. The authors of Ref. 14 were the first to write the working equations in dimensionless form and to introduce variables close to those used here.

Similarity techniques play an important role in the numerical modeling of processes occurring in FEL amplifiers. In the one-dimensional approximation the output characteristics of the amplifier are determined by a set of eight parameters:

$$l, \kappa_0, \omega, \mathscr{E}_0, j_0, H_0, \langle (\Delta\mathscr{E})^2 \rangle, E_{ext},$$

where l is the undulator length. It follows from the equations that the set of similar operating regimes of the FEL amplifier and all the dimensionless combinations formed from the various physical quantities are determined by the values of the five dimensionless parameters

$$\Lambda_0 l, \hat{C}, \hat{\kappa}_p^2, \hat{\Lambda}_T^2, E_{ext}/E_0.$$

Here E_0 is new normalization factor arising in the description of the nonlinear regime. The combination E_f/E_0, where E_f is the amplitude of the wave field at the amplifier output, is dimensionless. Therefore, in the general case we can write

$$E_f/E_0 = \mathscr{D}(\Lambda_0 l, \hat{C}, \hat{\kappa}_p^2, \hat{\Lambda}_T^2, E_{ext}/E_0).$$

The universal function $\mathscr{D}$ can be calculated by numerically solving the dimensionless self-consistent field equations.

The system of working equations

The equation describing the variation of the particle energy $\mathscr{E}$ as a function of the coordinate z along the undulator axis can be obtained from the Hamiltonian H written in the variables $\mathscr{E}$ and $\psi = \kappa_0 z + \omega(z/c - t)$ corresponding to the energy and the longitudinal phase canonically conjugate to it. In first order in the expansion in the vector potential of the wave $A_\perp$ neglecting space-charge effects, the Hamiltonian (4) can be written as

$$H(\mathscr{E}, \psi, z) = \int^{\mathscr{E}} [\kappa_0 - \omega(v_z^{-1}(\mathscr{E}) - c^{-1})] d\mathscr{E} - \varphi \sin(\psi + \psi_0), \tag{40}$$

where $v_z(\mathscr{E})$ is the longitudinal component of the electron velocity in the undulator, $\varphi = (e\theta_0 E)$, and ψ_0 are, respectively, the amplitude and phase of the effective potential; and $E = |\partial \mathbf{A}_\perp/\partial(ct)|$ is the amplitude of the electric field of the amplified electromagnetic wave. The parameters φ and ψ_0 are related to the complex amplitude of the effective potential U as in Sec. 1: $(\varphi/2)\exp(i\psi_0) = U$. The equations of motion corresponding to the Hamiltonian (40) are written in the form

$$\left.\begin{aligned} d\mathscr{E}/dz &= -\partial H/\partial\psi = \varphi\cos(\psi+\psi_0); \\ d\psi/dz &= \partial H/\partial\mathscr{E} = \kappa_0 - \omega(v_z^{-1} - c^{-1}) \\ &\quad - \partial\varphi/\partial\mathscr{E}\,\sin(\psi+\psi_0). \end{aligned}\right\} \tag{41}$$

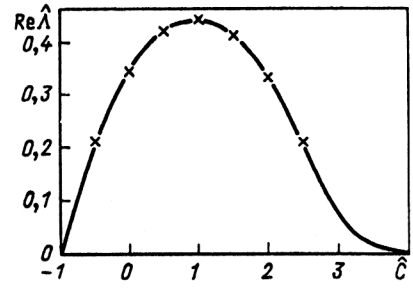

FIG. 9. The linear regime. Dependence of the normalized increment on the normalized detuning for $\hat{\Lambda}_T^2 = 0.5$ and $\hat{\kappa}_p^2 = 0$. The solid line is the result of solving Eq. (38), and the crosses are the result of numerical modeling using Eqs. (44) and (45).

From the Maxwell wave equation we easily find that, owing to the coherent radiation of the electron beam in the undulator, the amplitude and phase of the effective potential will vary as

$$\left.\begin{aligned} d\varphi/dz &= -(\pi m_0 c^2 \theta_0^2 I/I_A)\rho_1 \cos(\psi_0-\psi_1); \\ d\psi_0/dz &= (\pi m_0 c^2 \theta_0^2 I/I_A)(\rho_1/\varphi)\sin(\psi_0-\psi_1), \end{aligned}\right\} \quad (42)$$

where ρ_1 and ψ_1 are, respectively, the amplitude and phase of the first harmonic of the beam density ρ:

$$\rho_1 \cos\psi_1 = \frac{1}{\pi}\int_0^{2\pi} \rho\cos\psi d\psi,$$

$$\rho_1 \sin\psi_1 = -\frac{1}{\pi}\int_0^{2\pi} \rho\sin\psi d\psi.$$

The normalization of the function $\rho(z,\psi)$ is chosen in such a way that $I\rho$ can be interpreted as the longitudinal component of the current density of the beam. Here I is the average beam current. Equations (41) and (42) form a system of self-consistent equations for the FEL amplifier in the one-dimensional approximation.

For small deviations of the energy from the initial value, the Hamiltonian (40) takes the form

$$H = CP + \omega P^2/(2\gamma_z^2 \mathscr{E}_0 c) - \varphi\sin(\psi+\psi_0), \quad (43)$$

where $P=\mathscr{E}-\mathscr{E}_0$, and C is the detuning from resonance for a particle of energy $\mathscr{E}_0$:

$$C = \kappa_0 + \omega/c - \omega/v_z(\mathscr{E}_0) \cong \kappa_0 - \omega/(2c\gamma_z^2).$$

It is convenient to replace the variables z, P, φ, and ρ_1 by others proportional to them by setting $\hat{z}=\Lambda_0 z$, $\hat{P}=\omega P/(c\gamma_z^2 \mathscr{E}_0 \Lambda_0)$, $\hat{\varphi}=\omega\varphi/(c\gamma_z^2\mathscr{E}_0\Lambda_0^2)$, and $\hat{\rho}_1=\rho_1 S$. Here S is the cross-sectional area of the beam ($j_0=I/S$). As a result, Eqs. (41) and (42) can be rewritten as

$$\left.\begin{aligned} d\hat{P}/d\hat{z} &= \hat{\varphi}\cos(\psi+\psi_0); \\ d\psi/d\hat{z} &= \hat{P}+\hat{C}+\beta\hat{\varphi}\sin(\psi+\psi_0); \end{aligned}\right\} \quad (44)$$

$$\left.\begin{aligned} d\hat{\varphi}/d\hat{z} &= -\hat{\rho}_1\cos(\psi_0-\psi_1); \\ d\psi_0/d\hat{z} &= (\hat{\rho}_1/\hat{\varphi})\sin(\psi_0-\psi_1), \end{aligned}\right\} \quad (45)$$

where we have introduced the notation $\beta = c\gamma_z^2\Lambda_0/\omega$. The parameter β is inversely proportional to the number of undulator periods on the characteristic distance over which the wave field grows in the linear regime and is always small. Therefore, the terms proportional to β can be neglected in the second equation of the system (44).

The numerical-modeling algorithm

We split the electron beam into a large number of layers perpendicular to the axis. Let there be N layers in the wavelength at which the beam is modulated, i.e., in the interval of the phase ψ from 0 to 2π. The beam density function $\hat{\rho}$ periodic in the phase ψ in the phase interval $(0,2\pi)$ can be written as

$$\hat{\rho} = \frac{2\pi}{N}\sum_{j=1}^{N}\delta(\psi-\psi_{(j)}), \quad (46)$$

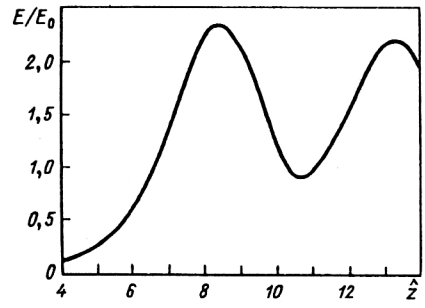

FIG. 10. The nonlinear regime. Dependence of the normalized field amplitude on the normalized undulator length for $\hat{C}=0$, $\hat{\kappa}_p^2=0$, $\hat{\Lambda}_T^2=0$, and $E_{ext}/E_0=0.01$.

where $\psi_{(j)}$ is the phase of the jth layer and $\delta(\psi-\psi_{(j)})$ is the delta function. According to the definition (46), the function $\hat{\rho}$ is normalized by the condition

$$\int_0^{2\pi}\hat{\rho}d\psi = 2\pi.$$

The relation between the amplitude of the first harmonic of the beam density $\hat{\rho}_1$ and the function $\hat{\rho}$ is given by the expressions

$$\rho_1\cos\psi_1 = \frac{1}{\pi}\int_0^{2\pi}\hat{\rho}\cos\psi d\psi = \frac{2}{N}\sum_{j=1}^{N}\cos\psi_{(j)},$$

$$\hat{\rho}_1\sin\psi_1 = -\frac{1}{\pi}\int_0^{2\pi}\hat{\rho}\sin\psi d\psi = -\frac{2}{N}\sum_{j=1}^{N}\sin\psi_{(j)},$$

where ψ_1 is the phase of the first density harmonic.

The equations of motion (44) applied to all N layers together with the field equations (45) give a system of $2N+2$ equations. By solving them numerically it is possible to study the nonlinear operating regime of the FEL amplifier. Let an unmodulated electron beam and an electromagnetic wave of amplitude E_{ext} be fed to the undulator input. Then the initial conditions for $z=0$ will be

$$\hat{P}_i(0)=0, \quad \rho_1(0)=0, \quad \hat{\varphi}(0)=\hat{\varphi}_{ext}=E_{ext}/E_0,$$

where the parameter E_0, according to the definition of $\hat{\varphi}$, is $E_0=(c\gamma_z^2\mathscr{E}_0\Lambda_0^2)/(e\omega\theta_0)$. The dependence of the normalized amplitude of the field $\hat{\varphi}$ on the normalized undulator length $\hat{z}$ for $\hat{C}=0$ and $\hat{\varphi}_{ext}=0.01$, found by the method described above, is shown in Fig. 10. The field stops growing in the saturation regime of the amplifier, when the beam is overmodulated and a significant fraction of the electrons begin to be accelerated by the effective potential. The maximum value of the normalized amplitude of the field for $\hat{C}=0$ is

$$\hat{\varphi}_{max}=E_{max}/E_0=2.34$$

and for high gain, i.e., when $E_{ext}/E_0 \ll 1$, it is independent of the field amplitude at the amplifier input.

Power conservation in the interaction between the electron beam and the electromagnetic wave in the undulator

The coefficient characterizing the transformation of beam energy into radiation (the efficiency) for high gain can be defined as the ratio of the flux density of the radiation power at the amplifier output to the flux density of the electron beam power at the input. In the one-dimensional approximation that we are using, the average power transported by the wave is given by

$$W=cE^2S/(4\pi).$$

Therefore, the efficiency of the amplifier in the limit $G\gg 1$ is found from the expression

$$\eta=eW/(\mathscr{E}_0 I)=\beta\hat{\varphi}^2/4. \tag{47}$$

The electromagnetic power radiated by the electron beam in the undulator must be equal to the difference of the kinetic-energy fluxes at the input and output of the amplifier, i.e., $W=-\langle P\rangle I/e$, where $\langle P\rangle$ is the average change of the energy of the beam particles. Therefore, using the power conservation law, we can define the amplifier efficiency as the ratio of the average change of energy of the beam particles $\langle P\rangle$ to the nominal energy $\mathscr{E}_0$: $\eta=-\langle P\rangle/\mathscr{E}_0$. Now we transform to the dimensionless quantity $\langle\hat{P}\rangle$. Then the expression for the efficiency will take the form $\eta=-\beta\langle\hat{P}\rangle$. In the macroparticle model we have

$$\langle d\hat{P}/dz\rangle=\hat{\varphi}N^{-1}\sum_{j=1}^{N}\cos(\psi_{(j)}+\psi_0).$$

Here we have used the first canonical equation of motion of the particles in the wave field (44). The sum in the latter can be expressed in terms of the amplitude and phase of the first harmonic of the beam density, using the expression

$$N^{-1}\sum_{j=1}^{N}\cos(\psi_{(j)}+\psi_0)=(1/2)\hat{\rho}_1\cos(\psi_1-\psi_0).$$

Using the first equation of the system (45), we obtain

$$\langle d\hat{P}/d\hat{z}\rangle=-\hat{\varphi}(1/2)d\hat{\varphi}/d\hat{z}.$$

From this it follows that

$$\eta=-\beta\langle\hat{P}\rangle=\beta\hat{\varphi}^2/4.$$

Comparison with Eq. (47) shows that the power conservation condition is satisfied. In the special case of tuning to resonance ($\hat{C}=0$), from Eq. (47) we obtain the following simple expression for the reduced maximum efficiency of the FEL amplifier:

$$\eta_{\max}/\beta=1.37.$$

Saturation in FEL amplifiers with high gain

When the amplifier has normalized length $\hat{z}>4$, the power gain in the saturation regime for $\hat{C}=0$ can be calculated from the following expression with an error of a few percent:

$$G_{\max}=(1/38)\exp(\sqrt{3}\Lambda_0 z), \tag{48}$$

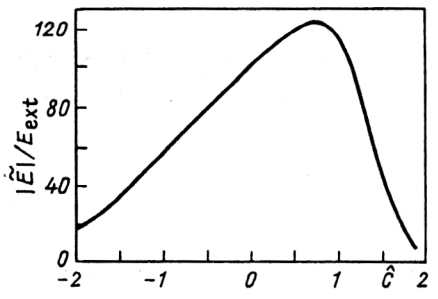

FIG. 11. The nonlinear regime. Dependence of the field amplitude at the amplifier output, normalized to the amplitude of the input signal, on the normalized detuning $\hat{C}$ for $\hat{\kappa}_p^2=0$, $\hat{\Lambda}_T^2=0$, $\hat{z}=7.4$, and $E_{ext}E_0=2.34\times10^{-2}$. Exactly on resonance ($\hat{C}=0$) the amplifier operates in the saturation regime.

or, in decibels, $G_{\max}(\mathrm{dB})=10\log(G_{\max})=7.5\Lambda_0 z-15.8$. The field amplitude at the amplifier input E_{ext} at which the saturation regime is reached is found from the expression

$$E_{ext}/E_0=2.34/\sqrt{G_{\max}}, \tag{49}$$

with G given by Eq. (48). It should be noted that using the graph shown in Fig. 10, we can calculate the change of the amplitude of the wave field along the undulator axis for any amplifier with normalized length $\hat{z}>4$ operating in the saturation regime for $\hat{C}=0$. The point where the field reaches its maximum at $\hat{z}=8.4$ in Fig. 10 corresponds to the amplifier output, i.e., according to (48) and (49), to the point with coordinate equal to

$$\hat{z}_{\max}=\Lambda_0 z_{\max}=3.1+2(3)^{-1/2}\ln(E_0/E_{ext}). \tag{50}$$

The field amplitude at a point lying a distance $\hat{z}=\hat{z}_{\max}-\Delta\hat{z}$ from the amplifier input is equal to the field amplitude in Fig. 10 for $\hat{z}=8.4-\Delta\hat{z}$. Starting with $\Delta\hat{z}>4$ the linear approximation becomes applicable, and the amplitude E can be found using Eq. (25) with E_{ext} in it found from Eqs. (48) and (49).

An important output characteristic of the amplifier is also the bandwidth of the amplification in the saturation regime. Let us consider a specific example. Let the normalized length of the amplifier be $\hat{z}=7.4$. Then, according to Eqs. (48) and (49), exactly on resonance the saturation regime is reached for the input amplitude $E_{ext}=2.34\times10^{-2}E_0$, and the gain is $G=40$ dB. The dependence of the field amplitude at the output of such an amplifier on the detuning parameter is shown in Fig. 11. In this case the amplification bandwidth is $\Delta\hat{C}=1.54$. The graph in Fig. 12 can be used to find $\Delta\hat{C}$ for an amplifier operating in the saturation regime for $\hat{C}=0$ and having a different value of the gain G (i.e., a different normalized length).

In the general case, for any value of the detuning parameter satisfying the condition $\hat{C}<1.89$, there exists a value of the input amplitude E_{ext} for which the output amplitude reaches a maximum. The maximum efficiency of the amplifier $\eta_{\max}$ is a universal function of the detuning parameter $\hat{C}$. A graph of this function is shown in Fig. 13.

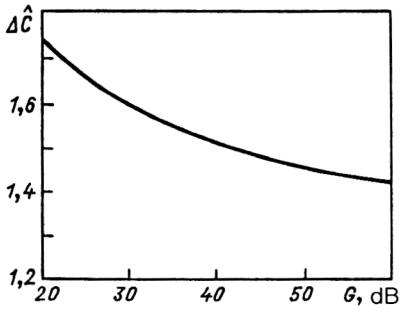

FIG. 12. The nonlinear regime. Dependence of the normalized bandwidth of the amplification on the power gain for $\hat{\kappa}_p^2=0$ and $\hat{\Lambda}_T^2=0$. Exactly on resonance ($\hat{C}=0$) the amplifier operates in the saturation regime.

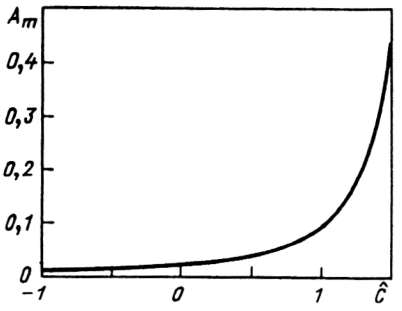

FIG. 14. The nonlinear regime. Dependence of the pre-exponential factor in Eq. (51) on the normalized detuning.

We see that the maximum efficiency of the amplifier is a growing function of the detuning parameter.

The power gain in the saturation regime is also a universal function of the parameter $\hat{C}$:

$$G_{\max}=A_m(\hat{C})\exp[2\,\mathrm{Re}(\hat{\Lambda})\hat{z}]. \qquad (51)$$

A graph of the function $A_m(\hat{C})$ is shown in Fig. 14. The values of the normalized increment are found using the graph in Fig. 2. The amplitude of the input signal at which the saturation regime is reached can be determined using the graphs in Figs. 2, 13, and 14 and the expression

$$E_{\text{ext}}/E_0=2[\eta_{\max}/(\beta G_{\max})]^{1/2}.$$

In practical situations it is often important to know how the field amplitude varies at the amplifier output as the input amplitude is varied. The dependence of E on E_{ext} for an amplifier operating in the saturation regime for $\hat{C}=0$ is shown in Fig. 15. It should be noted that for high gain the amplitude characteristic of the amplifier is independent of the gain. The admissible pulsations of the beam current can be determined using Fig. 16, where we give graphs of the dependence of the field amplitude at the amplifier output on the beam current for different values of the gain G.

The number of layers N in the numerical modeling procedure is often taken to be 200 to 400. Here the results of calculations for the nonlinear regime are independent of the actual value of N to within an error of 0.1%. The programs have been tested by numerical modeling of the linear regime. In Fig. 2 we compare the values of the increment obtained by numerical modeling with the values obtained by solving the characteristic equation (26). In Fig. 4 we compare the amplitude–frequency characteristic of the amplifier obtained by numerical modeling with the results of the analytic solution of the initial-value problem using Eq. (23). We see that there is good agreement between the numerical and analytical results. For $N=200$ macroparticles the discrepancy is less than 0.1%.

Space-charge effects in the saturation regime

To carry out a comprehensive numerical modeling of the processes occurring in FEL amplifiers, the macroparticle equation of motion (44) must be supplemented by the corresponding term determining the effect of the space-charge field. In the model that we are analyzing the electron beam is represented as charged layers of zero length in the longitudinal direction. There are N layers within the wavelength λ of the beam density modulation. The surface charge density of each layer is $\sigma_q=j_0\lambda(v_zN)$. We transform to a comoving reference frame to find the longitudinal component of the space-charge electric field generated by the system of charged layers. In this approximation the

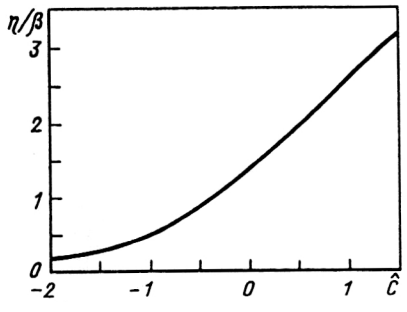

FIG. 13. The nonlinear regime. Dependence of the normalized efficiency of the amplifier in the saturation regime on the normalized detuning for $\hat{\kappa}_p^2=0$ and $\hat{\Lambda}_T^2=0$.

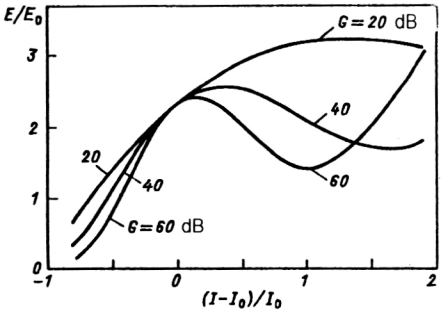

FIG. 15. The nonlinear regime. Dependence of the normalized field amplitude at the amplifier output on the field amplitude at the input, normalized to the optimal E_{ext}^m. The saturation regime is realized for $E_{\text{ext}}=E_{\text{ext}}^m$. Here $\hat{C}=0$, $\hat{\kappa}_p^2=0$, and $\hat{\Lambda}_T^2=0$.

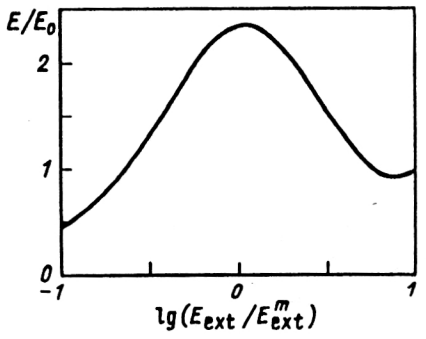

FIG. 16. The nonlinear regime. Dependence of the normalized field amplitude at the amplifier output on the change of the beam current for various values of the power gain. The saturation regime is realized for $I=I_0$. Here $\hat{C}=0$, $\hat{\kappa}_p^2=0$, and $\hat{\Lambda}_T^2=0$. The field amplitude is normalized at the current $I=I_0$.

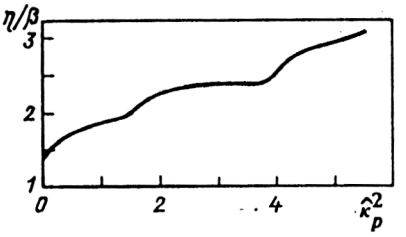

FIG. 17. The nonlinear regime. Dependence of the normalized efficiency of the amplifier in the saturation regime on the space-charge parameter $\hat{\kappa}_p^2$ for tuning to the maximum increment. The parameter $\hat{C}=\hat{C}_m(\hat{\kappa}_p^2)$ is determined using the graph in Fig. 5, and $\hat{\Lambda}_T^2=0$.

motion of the layers in the comoving frame is nonrelativistic, and the space-charge electric field can be calculated in the quasistatic approximation.

We consider two reference frames. One, K, is stationary and the other, K', moves relative to the first along the z axis with rectilinear motion at speed v_z equal to the speed of the beam particle at the undulator input. To calculate the space charge it is necessary to know the positions of the layers along the z axis both behind and in front of the observation point. The characteristic length scale over which the space-charge field is formed in this model is the wavelength $\lambda'=\gamma_z\lambda$. In our approximation the characteristic length over which the beam density varies is much larger than λ'. Therefore, in finding the field generated by the system of charged layers at a given observation point z', we can assume that these layers are arranged periodically with period λ'. The position of the layers within a wavelength is a function of the coordinate z' and the time t'.

The quasistatic potential of the system of charged layers located throughout the distance λ' in the frame K' is defined as

$$V_q'=2\pi\sigma_q\int_0^\infty rdr\int_{-\infty}^{\infty}d\zeta\rho'(\zeta)[r^2+(z'-\zeta)^2]^{-1/2},$$

$$\rho'(\zeta)=\sum_{-\infty}^{\infty}\delta(\zeta-n\lambda')$$

$$=(1/\lambda')\sum_{-\infty}^{\infty}\exp(2\pi in\zeta/\lambda').$$

After simple transformations we find

$$V_q'=2\sigma_q k'\sum_1^\infty\cos(nk'z')\int_0^\infty rdr\int_{-\infty}^{\infty}d\zeta\cos(nk'\zeta)$$
$$\times[r^2+\zeta^2]^{-1/2}.$$

Here $k'=2\pi/\lambda'$. We have discarded the term with $n=0$. It describes the potential of uniformly charged space and is not of interest for our discussion. Using integral tables, we obtain

$$V_q'=\frac{4\sigma_q}{k'}\sum_1^\infty\frac{\cos(nk'z')}{z^2}.$$

Accordingly, for the electric field we have

$$E_z=-\frac{dV_q'}{dz'}=4\sigma_q\sum_1^\infty\frac{\sin(nk'z')}{z}.$$

Using the well known mathematical formula

$$\sum_1^\infty\frac{\sin(n\xi)}{n}=\frac{\pi-\xi}{2}\quad(0<\xi<2\pi),$$

we find that the field E_z will vary with z' in the range $0\leqslant z'\leqslant\lambda'$ as

$$E_z=2\pi\sigma_q(1-2z'/\lambda').$$

From this we find the expression for the space-charge field at the ith layer:

$$E_i=2\sigma_q\sum_{j\neq i}[\pi\,\mathrm{sgn}\,(\psi_{(i)}-\psi_{(j)})-(\psi_{(i)}-\psi_{(j)})].$$

Here $\psi_{(i)}$ and $\psi_{(j)}$ are the phases of the ith and jth layers,

$$\mathrm{sgn}(\psi_{(i)}-\psi_{(j)})=1\quad\text{for}\quad(\psi_{(i)}-\psi_{(j)})>0,$$

$$\mathrm{sgn}(\psi_{(i)}-\psi_{(j)})=-1\quad\text{for}\quad(\psi_{(i)}-\psi_{(j)})<0.$$

Using the expression for the Hamiltonian (5), we find that the inclusion of the effect of the space-charge field in this case reduces to the addition of the term $eE_z(\psi,z)$ to the right-hand side of the first equation of the system (44). Finally, the equations of motion of the ith layer are written in the following normalized form:

$$\frac{d\hat{P}_i}{d\hat{z}}=\hat{\varphi}\cos(\psi_{(i)}+\psi_0)+\hat{\kappa}_p^2\left\{\frac{1}{N}\sum_{j\neq1}[\pi\,\mathrm{sgn}(\psi_{(i)}\right.$$
$$\left.-\psi_{(j)})-(\psi_{(i)}-\psi_{(j)})]\right\},$$
$$d\psi_{(i)}/d\hat{z}=\hat{P}_i+\hat{C}.\qquad(52)$$

When the space-charge effect is taken into account, the maximum efficiency of the amplifier is a universal function of two parameters, the detuning parameter $\hat{C}$ and the space-charge parameter $\hat{\kappa}_p^2$. In the special case where the parameter $\hat{C}$ is chosen such that the growth increment of the field in the linear regime reaches its maximum, the

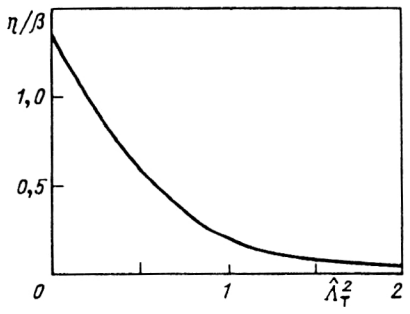

FIG. 18. The nonlinear regime. Dependence of the normalized efficiency of the amplifier in the saturation regime for tuning to the maximum increment on the energy-spread parameter $\hat{\Lambda}_T^2$; $\hat{\kappa}_p^2 = 0$, and the parameter $\hat{C} = \hat{C}_m(\hat{\Lambda}_T^2)$ is determined using the graph in Fig. 8.

amplifier efficiency in the saturation regime is a universal function of only the single parameter $\hat{\kappa}_p^2$. This dependence is shown in Fig. 17. We see from this figure that the maximum efficiency of the amplifier is a growing function of the space-charge parameter.

Numerical modeling of the linear regime was used to test the computational program for the nonlinear regime, taking into account the space-charge effect. In Figs. 6 and 7 we compare the results of the numerical and analytic calculations. When the number of macroparticles (layers) in the interval of the phase ψ from 0 to 2π is $N=200$, the results of the numerical modeling coincide with the analytic results with better than 0.1% accuracy.

Energy-spread effects in the saturation regime

When the beam has a Gaussian energy spread, the maximum efficiency of the amplifier is a universal function of the three parameters $\hat{C}$, $\hat{\kappa}_p^2$, and $\hat{\Lambda}_T^2$. In the special case where $\hat{\kappa}_p^2 \to 0$ and the detuning parameter is $\hat{C}_m$, where the increment reaches its maximum, the efficiency of the amplifier in the saturation regime is a function of the single parameter $\hat{\Lambda}_T^2$. A graph of this function is given in Fig. 18. From it we see that the energy spread leads to a sharp drop in the amplifier efficiency.

The energy spread of the beam was included in the numerical modeling of the nonlinear regime by dividing all the macroparticles in the phase interval $0 \leqslant \psi \leqslant 2\pi$ for $z = 0$ into a small even number of groups. The macroparticles in each group have identical phases ψ for $z=0$. The initial values of the normalized moments $\hat{P}_i$ of the particles in each group are described by a Gaussian distribution with rms deviation $\langle (\Delta\hat{P})^2 \rangle = 2\hat{\Lambda}_T^2$. The phases of the groups of particles for $z=0$ were distributed in the interval from 0 to 2π in such a way that the amplitude of the first harmonic of the macroparticle density was equal to zero.

The program was tested by numerical modeling of the linear regime. In Figs. 7 and 9 we compare the analytic and numerical solutions of the self-consistent field equation in the high-gain limit. The solid lines are calculated using the analytic expressions (37) and (38), and the crosses are the results of numerical calculations using Eqs. (45) and (52). In the numerical modeling the initial number of subdivisions in the phase ψ in the interval between 0 and 2π was taken to be 8. The number of macroparticles for modeling the spread in each of the eight groups was taken to be 200. We see from the figures that there is good agreement between the numerical and analytic results.

3. OPTIMIZATION OF THE POWER OUTPUT OF THE FEL AMPLIFIER BY VARIATION OF THE UNDULATOR PARAMETERS

Preliminary remarks

The operation of the FEL amplifier is based on the prolonged (resonance) interaction of the electron beam with the electromagnetic wave in the undulator. Therefore, the parameter Λ_0/κ_0, which is proportional to the inverse number of undulator periods in the characteristic rise length, is always much less than unity. The decrease of the electron velocity due to electron deceleration by the wave field leads to violation of the synchronism between the particles and the wave, as a result of which the amplifier efficiency turns out to be limited to be a value of order Λ_0/κ_0.

A promising method of raising the efficiency of an FEL amplifier is by variation of the undulator parameters along the undulator axis. This allows the preservation of the synchronism required for the amplifier operation and raises the efficiency to a value of order unity. This technique of raising the efficiency of FEL amplifiers was first suggested in Ref. 8. Later, numerical modeling was used to carry out calculations of the efficiency of an amplifier with varying undulator parameters.[9,10]

The FEL amplifier with optimal undulator (the low-efficiency approximation). Technique for calculating the optimal undulator parameters

According to the system of equations (44), the particle motion is determined by the detuning parameter

$$C = \kappa_0 - \omega/2c\gamma_z^2 = \kappa_0 - \omega(1+Q^2)/(2c\gamma^2),$$

which is a function of the undulator period $\lambda_0 = 2\pi/\kappa_0$ and the parameter describing the magnetic force $Q = eH_0/(m_0c^2\kappa_0)$. Variation of the undulator parameters causes the detuning parameter to become a function of the coordinate z. We consider one of the possible methods of varying the undulator parameters, namely, variation of the period λ_0 for constant magnetic-force parameter $Q = \text{const}$. The latter condition implies that the field H_0 on the undulator axis must vary as the inverse of the period ($H_0 \propto \lambda_0^{-1}$).

According to Ref. 11, in the case of a helical undulator with bifilar winding, the field on the axis is (in SI units)

$$H_0 = I_s(\pi R)^{-1}[\kappa_0^2 R^2 K_0(\kappa_0 R) + (\kappa_0 R)K_1(\kappa_0 R)],$$

where I_s and R are, respectively, the current and radius of the helical winding, and K_0 and K_1 are second-order modified Bessel functions. The magnetic-force parameter Q for constant current in the winding ($I_s = \text{const}$) for such an undulator is a universal function of the parameter $\kappa_0 R$. Therefore, the variation of the undulator period for con-

stant Q in this case is realized by shaping the windings to be proportional to the period, i.e., $R \propto \lambda_0$.

First we assume that the amplifier efficiency is increased many times by variation of the undulator parameters, but still remains much smaller than unity. This approximation is not only of methodological but also of practical interest, since the amplifier length grows considerably with increasing efficiency, and under real conditions in many cases it is necessary to impose the limit, for example, that the efficiency increases from $\eta = 1\%$ to $\eta = 10\%$ and no more. When numerical modeling is used, the condition that η be small means that the system of normalized equations (44), (45) can be used, as in the above calculation of the nonlinear regime of the FEL amplifier with constant undulator parameters. The detuning parameter C in the second equation of the system (44) is now a given function of z and is expressed for $Q = \text{const}$ in terms of the variation of the undulator wave number κ_0 as $C = C(0) + \Delta\kappa_0$.

Let us consider the method of varying the undulator parameters in which the detuning is a constant in the initial section of the undulator and then, beginning at some distance, grows smoothly and monotonically as a quadratic polynomial:

$$C(z) = C(0) + \Delta\kappa_0(z)$$
$$= \alpha_0 + \alpha_1(z - z_i) + \alpha_2(z - z_i)^2,$$

where z_i is the point where the variation begins. The parameter $\hat{C}$ in Eqs. (44) can be rewritten in normalized form as

$$\hat{C} = k_0 + k_1(\hat{z} - \hat{z}_i) + k_2(\hat{z} - \hat{z}_i)^2,$$
$$\hat{z}_i = \Lambda_0 z_i, \quad k_0 = \alpha_0/\Lambda_0, \quad k_1 = a_1/\Lambda_0^2, \quad k_2 = a_2/\Lambda_0^3. \tag{53}$$

The choice of this type of variation of the detuning is easily understood when it is recalled that the amplitude of the radiation field of a completely bunched electron beam in the undulator exactly on resonance must grow in proportion to the undulator length, according to Eqs. (45). From the power balance condition (47) it follows that the variation of the particle energy for constant tuning to resonance must be proportional to the squared length of the radiation section. In the low-efficiency approximation we see from the particle equations of motion (44) that for the synchronicity condition to be satisfied, the detuning parameter $\hat{C}$ should compensate for the change in the particle beam energy. These heuristic arguments suggest the formulation of the following restriction on the function $\hat{C}(\hat{z})$. For any type of variation of the undulator parameters leading to the capture of beam particles into the coherent bremsstrahlung regime, the asymptote of $\hat{C}(\hat{z})$ must be a quadratic function of the undulator length. There are many ways of varying the undulator parameters which satisfy this condition. The variation that we use is simplest and requires the optimal selection of only the four coefficients k_0, k_1, k_2, and $\hat{z}_i$. The coefficient selection was done using a program of optimization to the field maximum for

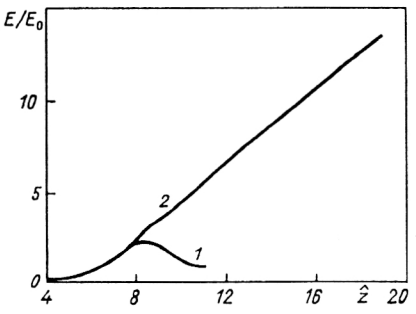

FIG. 19. Parameter variation. Dependence of the normalized field amplitude on the normalized undulator length. Here $\hat{C}=0$, $\hat{\kappa}_p^2 = 0$, $\hat{\Lambda}_T^2 = 0$, and $E_{ext}/E_0 = 0.01$. Curve 1 is for the case without parameter variation, and curve 2 is for the case of variation of the detuning parameter according to the law $\hat{C}=0$ for $\hat{z}<7$ and $\hat{C}=1.44(\hat{z}-7)+0.36(\hat{z}-7)^2$ for $\hat{z}>7$.

$$(\hat{z} - \hat{z}_i) \gg 1.$$

We obtained the values

$$k_0 = 0, \quad k_1 = 1.44, \quad k_2 = 0.36. \tag{54}$$

The optimal length of the undulator section with constant parameters is determined from the condition

$$\hat{z}_i = 1.7 + 2(3)^{-1/2} \ln(E_0/E_{ext}). \tag{55}$$

Comparing Eqs. (50) and (55), we conclude that the variation should start before reaching a distance $\Delta z = 1.4/\Lambda_0$ to the maximum of the field in the undulator with constant parameters. The coefficient of particle capture into the bremsstrahlung regime for the values of the coefficients in (54) and (55) is 65%.

The coefficient of particle capture into the coherent-bremsstrahlung regime when the undulator parameters are varied according to the law (53) strongly depends on the value of the coefficient k_2. For $k_2 > 0.4$ there is no particle capture into the coherent-bremsstrahlung regime and no significant increase of the efficiency. When k_2 is changed to values below 0.36, the coherent-bremsstrahlung regime remains stable, and the capture coefficient is even increased slightly. However, the equilibrium bremsstrahlung phase of the entrapped particles moves closer to 90°, which causes the field amplitude to increase more slowly than for $k_2 = 0.36$.

The technique for calculating the output characteristics of the optimized FEL amplifier

In Fig. 19 we show a graph of the normalized amplitude $E(\hat{z})/E_0$ for the case where $E_{ext}/E_0 = 0.01$. The variation of the undulator parameters begins at $\hat{z}_i = 7$ and follows the law

$$C/\Lambda_0 = 1.44(\hat{z} - 7) + 0.36(\hat{z} - 7)^2.$$

For comparison, in Fig. 19 we also show the dependence $E(\hat{z})/E_0$ for the undulator with constant parameters.

The graph in Fig. 19 can be used to calculate the variation of the field amplitude along the undulator axis for an arbitrary value of E_{ext}/E_0. In fact, up to the value $\hat{z} = \hat{z}_i$

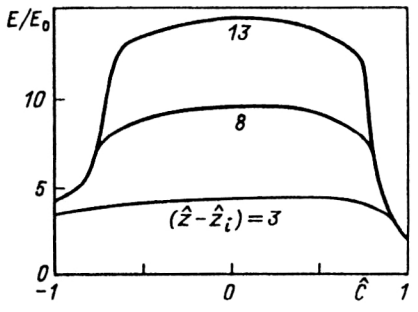

FIG. 20. Parameter variation. Dependence of the normalized field amplitude at the amplifier output in the low-efficiency regime on the normalized initial detuning for various lengths of the bremsstrahlung section. Here $\hat{\kappa}_p^2=0$ and $\hat{\Lambda}_T^2=0$.

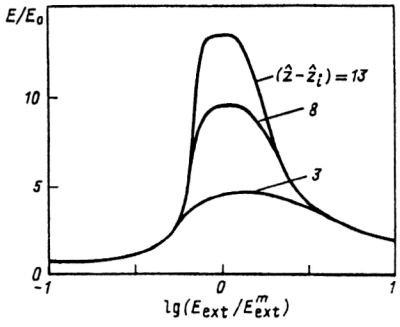

FIG. 22. Parameter variation. Dependence of the normalized field amplitude at the amplifier output on the field amplitude at the input, normalized to E_{ext}^m. The coordinate $\hat{z}_i$ of the beginning of the variation section is calculated for $E_{ext}=E_{ext}^m$, $\hat{\kappa}_p^2=0$, and $\hat{\Lambda}_T^2=0$.

given by Eq. (55), the function $E(\hat{z})/E_0$ can in general be found as described in Sec. 2. above. Then the point with coordinate $\hat{z}_i$ is put into correspondence with the point in Fig. 19 at $\hat{z}=7$, and the value of the normalized field amplitude at the point with coordinate $\hat{z}=\hat{z}_i+\Delta\hat{z}$ is equal to the value $E(7+\Delta\hat{z})/E_0$ in Fig. 19.

In the general case the variation of the field amplitude in the undulator with parameters varying as in Eqs. (53)–(55) can, for $(\hat{z}-\hat{z}_i)>3$, be calculated from the approximate expression

$$E(\hat{z})/E_0=\hat{\varphi}(\hat{z})=\hat{z}-2(3)^{-1/2}\ln(E_0/E_{ext}). \quad (56)$$

We recall that the results given above are valid when the efficiency is small at the amplifier output for $\hat{z}=\hat{z}_f$, i.e.,

$$\eta=[\hat{\varphi}(\hat{z}_f)]^2\beta/4\ll 1.$$

In Fig. 20 we show graphs of the dependence of the field amplitude at the amplifier output on the initial detuning $\hat{C}$ for various lengths of the bremsstrahlung section. The gain G on the segment of the undulator with constant parameters here is $G=40$ dB. The initial detuning C is

$$C=\kappa_0(0)-\omega(1+Q^2)m_0^2c^3/(2\mathscr{E}_0^2),$$

where $\kappa_0(0)$ is the initial value of the undulator wave number. We see from Fig. 20 that as the efficiency of the amplifier increases, the amplification bandwidth remains practically the same as in the saturation regime, so that the restrictions on the pulsations of the beam energy remain unchanged. These restrictions can be obtained using Fig. 21, in which we give graphs of the dependence of the field amplitude at the amplifier output on the beam current for various values of the length of the bremsstrahlung section. Here the deviation of the beam current is $\Delta I=I-I_0$, and the normalization factors are calculated for the current equal to I_0. We see from this figure that the coherent-bremsstrahlung regime remains stable for significant deviations of the beam current toward higher values. This is explained by the fact that, according to Eq. (53), an increase of the beam current keeping the other parameters of the problem fixed actually leads to a decrease of the coefficient k_2, which, as mentioned above, still satisfies the condition for the existence of particle capture in the coherent-bremsstrahlung regime. The amplitude characteristics of an amplifier with parameter variation are shown in Fig. 22.

The electron energy distribution at the output of the FEL amplifier

In practice it is often very important to know the energy distribution of the electrons in the beam at the ampli-

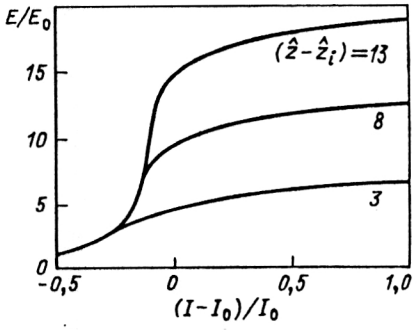

FIG. 21. Parameter variation. Dependence of the normalized field amplitude at the amplifier output in the low-efficiency regime on the change of the beam current for various lengths of the bremsstrahlung section. Here $\hat{C}=0$, $\hat{\kappa}_p^2=0$, and $\hat{\Lambda}_T^2=0$. The parameters are normalized at $I=I_0$.

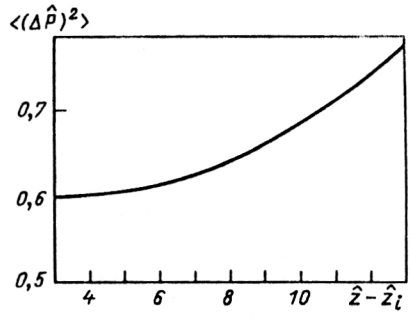

FIG. 23. Parameter variation. Dependence of the normalized rms energy spread of the entrapped particles on the length of the bremsstrahlung section in the low-efficiency regime.

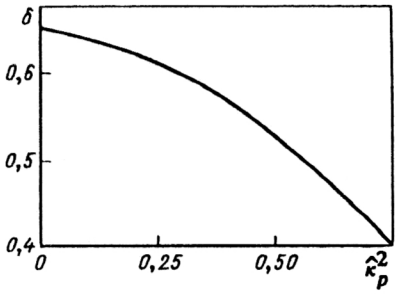

FIG. 24. Parameter variation. Dependence of the capture coefficient on the space-charge parameter in the low-efficiency regime for optimal variation of the undulator parameters. The energy-spread parameter is zero.

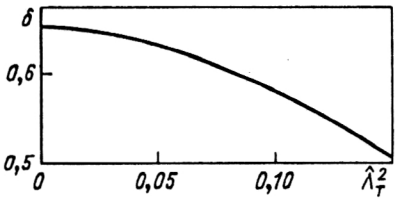

FIG. 25. Parameter variation. Dependence of the capture coefficient on the energy-spread parameter in the low-efficiency regime for optimal variation of the undulator parameters. The space-charge parameter is zero.

fier output. In Fig. 23 we show a graph of the dependence of the rms spread of the normalized momenta of the captured particles on the normalized length of the bremsstrahlung section. We see from this figure that the spread in the particle energies grows slowly during the bremsstrahlung process. This is explained by the fact that there is conservation of an adiabatic invariant in the phase oscillations of the captured particles. Assuming that the oscillations are linear, this invariant is $(\delta\hat{P})^2/(2\kappa_s)$, where $\delta\hat{P}$ is the amplitude of the oscillations of the normalized particle momentum, and

$$\kappa_s=(\hat{\varphi}\sin(\psi_s-\psi_0))^{1/2}$$

is the reduced wave number of the phase oscillations. From this we can conclude that for constant bremsstrahlung phase $(\psi_s-\psi_0)$ an increase of the amplitude of the effective potential $\hat{\varphi}$ leads to an increase in the momentum spread proportional to $\hat{\varphi}^{1/4}$. The rms energy spread of the particles is calculated using the expression

$$\langle(\Delta\mathscr{E}^2\rangle/\mathscr{E}_0^2=\beta^2\langle(\Delta\hat{P})^2\rangle.$$

For a significant increase of η the average energy of the captured particles is

$$\bar{\mathscr{E}}=\mathscr{E}_0-0.38\beta\mathscr{E}_0E^2/E_0^2.$$

The rms energy spread of the particles which have not been captured and their average energy are practically independent of the length of the bremsstrahlung section and are equal to

$$\langle(\Delta\mathscr{E})^2\rangle/\mathscr{E}_0^2\cong 3\beta^2,\quad \bar{\mathscr{E}}\cong\mathscr{E}_0-0.45\beta\mathscr{E}_0.$$

Effect of the space charge and the energy spread on the electron capture coefficient in the coherent-bremsstrahlung regime

Studies of the space-charge effect in amplifiers with variable undulator parameters have shown that, as expected, there is a defocusing effect which decreases the coefficient describing capture into the coherent-bremsstrahlung regime. Optimization calculations were carried out using the system of self-consistent field equations in the low-efficiency approximation (45), (52). The variation was done as

$$\hat{C}=\hat{C}_m \quad \text{for} \quad \hat{z}<\hat{z}_i,$$

$$\hat{C}=\hat{C}_m+k_1(\hat{z}-\hat{z}_i)+k_2(\hat{z}-\hat{z}_i)^2 \quad \text{for} \quad \hat{z}>\hat{z}_i, \qquad (57)$$

where $\hat{C}_m$ is the value of the detuning parameter at which the increment reaches its maximum. In this case the optimization problem was simplified by keeping the initial value of the detuning parameter fixed and equal to $\hat{C}_m$. This choice is based on specific physical considerations and is close to the optimal value. The parameters k_1, k_2, and $\hat{z}_i$ were selected by means of a program of optimization to the field maximum for $\hat{z}-\hat{z}_i\gg 1$. Figure 24 demonstrates the variation of the capture coefficient as a function of the space-charge parameter for optimal variation of the undulator parameters.

We used Eqs. (44) and (45) to study the effect of the energy spread in the beam on the process of capture and coherent bremsstrahlung of the particles by the wave in an undulator with variable parameters. In carrying out the optimization calculations the undulator parameters were varied according to (57). The capture coefficient as a function of the spread parameter for optimal variation of the undulator parameters is shown in Fig. 25.

Limits on the applicability of the low-efficiency approximation

Above, we described the relative motion of particles in an electromagnetic field by the Hamiltonian (43) obtained from the Hamiltonian (40) by expansion in the small deviation $P=\mathscr{E}-\mathscr{E}_0$. This approximation can become invalid in the case of an undulator with parameter variation. Then it becomes necessary to describe the motion of the layers using Eqs. (41) and (42), obtained from the original Hamiltonian (40).

We normalize Eqs. (41) and (42) in the usual manner with the only refinement that all the normalization factors are calculated using the initial values of the beam and undulator parameters. As a result, taking into account the fact that the magnetic-force parameter is $Q=\text{const}$ and the rotation angle of the particles in the undulator depends on the particle energy as

$$\theta=\theta_0/(1+\Delta\mathscr{E}/\mathscr{E}_0)=\theta_0/(1+\beta\hat{P}),$$

we obtain the following system of working equations:

$$\frac{d\hat{P}}{d\hat{z}}=\frac{\hat{\varphi}}{1+\beta\hat{P}}\cos(\psi+\psi_0);$$

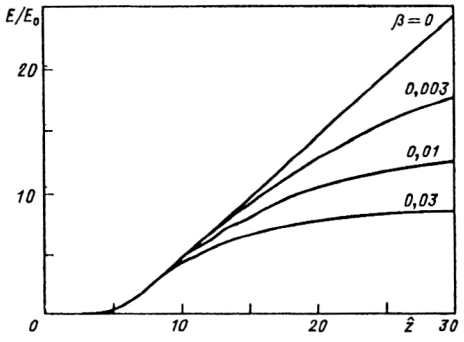

FIG. 26. Parameter variation. Dependence of the normalized field amplitude on the normalized undulator length for various values of the parameter β and $\hat{\kappa}_p^2=0$, $\hat{\Lambda}_T^2=0$, and $E_{ext}/E_0=0.01$. The normalized detuning varies as follows: $\hat{C}=0$ for $\hat{z}<7$ and $\hat{C}=1.44(\hat{z}-7)+0.36(\hat{z}-7)^2$ for $\hat{z}>7$.

$$\frac{d\psi}{d\hat{z}}=\frac{\hat{P}(1+\beta\hat{P}/2)}{(1+\beta\hat{P})^2}+\hat{C}+\beta\hat{\varphi}\frac{\sin(\psi+\psi_0)}{(1+\beta\hat{P})^2}. \tag{58}$$

Here, as before, the detuning parameter is

$$\hat{C}=\frac{\kappa_0(z)}{\Lambda_0}-\frac{m_0^2c^3\omega(1+Q^2)}{2\Lambda_0\mathscr{E}_0^2}.$$

The equations for $\hat{\varphi}$ and ψ_0 have the form

$$\left.\begin{aligned}\frac{d\hat{\varphi}}{d\hat{z}}&=-\frac{2}{N}\sum_{j=1}^{N}\frac{\cos(\psi_{(j)}+\psi_0)}{1+\beta\hat{P}_j},\\ \frac{d\psi_0}{d\hat{z}}&=\frac{1}{\hat{\varphi}}\left[\frac{2}{N}\sum_{j=1}^{N}\frac{\sin(\psi_{(j)}+\psi_0)}{1+\beta\hat{P}_j}\right].\end{aligned}\right\} \tag{59}$$

Let us first consider the situation where the undulator parameters are varied in such a way that the detuning function $\hat{C}$ is, as before, a quadratic polynomial, the coefficients of which have the values (54) and (55) optimal for the low-efficiency regime. I.e., for $\hat{z}>\hat{z}_i$ we have

$$\hat{C}=1.44(\hat{z}-\hat{z}_i)+0.36(\hat{z}-\hat{z}_i)^2.$$

The results of the numerical modeling of this case using the system of equations (58) and (59) are shown in Fig. 26 in the form of curves describing the dependence of the normalized field amplitude E/E_0 on the normalized undulator length $\hat{z}$ for various values of the parameter β. For relatively small lengths of the bremsstrahlung section the change of energy of the captured particles is small: $\Delta\mathscr{E}/\mathscr{E}_0=\beta\hat{P}\ll 1$. In this case the system of equations (58), (59) becomes the system (44), (45), and the graph of the function $\hat{\varphi}(\hat{z},\beta)$, shown in Fig. 26, coincides on this segment of the undulator with the graph of the function $\hat{\varphi}(\hat{z})$ in Fig. 19. At the beginning of the bremsstrahlung section the average momentum of the captured particles decreases quadratically with the undulator length, compensating for the quadratic increase of the parameter $\hat{C}$ in the equation for the phase ψ of the system (58), $d\psi/d\hat{z}=\hat{P}+\hat{C}$. Here the average variation of the phase of the captured particles is zero: $\langle d\psi/d\hat{z}\rangle=0$, and their motion corresponds to phase oscillations about the equilibrium bremsstrahlung phase $\psi_s-\psi_0=\text{const}$ (according to the second equation of the system (59), for $E/E_0\gg 1$ the change of phase of the effective potential ψ_0 can be neglected). As the length of the bremsstrahlung section is increased further, the difference between the approximate system of equations (44), (45) and the original system (58), (59) becomes important. According to the equation for the phase of the initial system,

$$\frac{d\psi}{d\hat{z}}=\frac{\hat{P}(1+\beta\hat{P}/2)}{(1+\beta\hat{P})^2}+\hat{C},$$

cancellation of the quadratic growth of the detuning parameter $\hat{C}$ will occur for slower stopping of the captured particles. Numerical modeling using the original system of equations (58), (59) shows that the number of captured particles does not change on the final bremsstrahlung section, and the particle motion corresponds to phase oscillations about the equilibrium bremsstrahlung phase $\psi_s-\psi_0$, which, in turn, undergoes a slow adiabatic decrease such that the phase difference $\psi_s-\psi_0$ approaches 90°. As a result, the growth of the field amplitude is slowed, and further increase of the undulator length becomes ineffective. The curves in Fig. 26 can be used to obtain some idea of the limits on the applicability of the coherent-bremsstrahlung regime considered above in the low-efficiency approximation. For example, from this figure we see that in the range of practical interest of the parameter β ($0.003<\beta<0.03$), the use of the results obtained with the approximate system of working equations (44), (45) is justified if the final amplifier efficiency is below 10%.

Calculations for FEL amplifiers with high efficiency

The results quoted above show that the efficient deep stopping of the captured particles requires variation of the undulator parameters such that the detuning parameter $\hat{C}$ increases with increasing length of the bremsstrahlung segment faster than the quadratic polynomial (53). It can be assumed on the basis of the form of the phase equation (58) that the linear law governing the rise of the field amplitude remains in force also in the deep stopping regime, if for $\hat{z}>\hat{z}_i=\hat{z}_m-1.4$ the detuning parameter is varied according to the law

$$\hat{C}=T(\hat{z})[1-\beta T(\hat{z})/2][1-\beta T(\hat{z})]^{-2},$$
$$T(\hat{z})=1.44(\hat{z}-\hat{z}_i)+0.36(\hat{z}-\hat{z}_i)^2. \tag{60}$$

The results of the numerical modeling confirm this assumption. In fact, when the parameter $\hat{C}$ is varied as in Eq. (60), the normalized field amplitude varies according to the linear law (56),

$$\hat{\varphi}(\hat{z},\beta)=\hat{\varphi}(\hat{z})\cong\hat{z}-\hat{z}_m+3,$$

even in the region where the amplifier efficiency becomes comparable to unity. The particle motion in the deep stopping regime is the following. The stopped particles execute phase oscillations about the equilibrium bremsstrahlung phase $\psi_s-\psi_0$, which nevertheless is slightly decreased, ap-

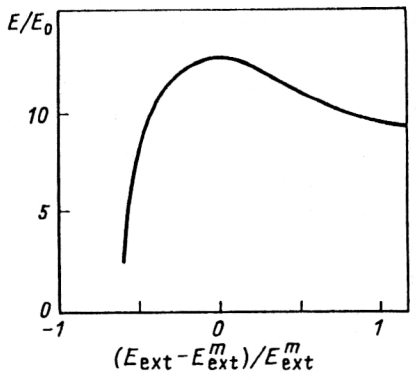

FIG. 27. Parameter variation. Dependence of the normalized field amplitude at the amplifier output in the high-efficiency regime on the variation of the field amplitude at the input. The normalized detuning varies as in Eq. (60), and the coordinate of the beginning of the variation section $\hat{z}_i$ is calculated for $E_{ext}=E^m_{ext}$. For $E_{ext}=E^m_{ext}$ the amplifier efficiency is $\eta=40\%$, and the power gain on the undulator section with constant parameters is 40 dB.

proaching 90°. This decrease of $\psi_s-\psi_0$ compensates for the slight increase in the beam emission, owing to the increase in the rotation angle of the captured particles.

Using Eqs. (47) and (56), we can calculate the total length z_f of the undulator required to attain the efficiency η:

$$z_f=\Lambda_0^{-1}[2(\eta/\beta)^{1/2}+2(3)^{-1/2}\ln(E_0/E_{ext})]. \quad (61)$$

The amplifier efficiency η must obviously be smaller than the capture coefficient, which is 65%. The total change of the undulator wave number according to Eq. (60) is

$$C=\Delta\kappa_0(z_f)$$
$$=2\pi[\lambda_0^{-1}(z_f)-\lambda_0^{-1}(z_i)]$$
$$=\Lambda_0 T(\hat{z}_f)[1-\beta T(\hat{z}_f)/2][1-\beta T(\hat{z}_f)]^{-2},$$

where $T(\hat{z}_f)$ and $\hat{z}_f=\Lambda_0 z_f$ are calculated from Eqs. (60) and (61).

In Figs. 27 and 28 we show the output characteristics of an amplifier with η equal to 40%. We see from these figures that when the amplifier efficiency is raised to a value

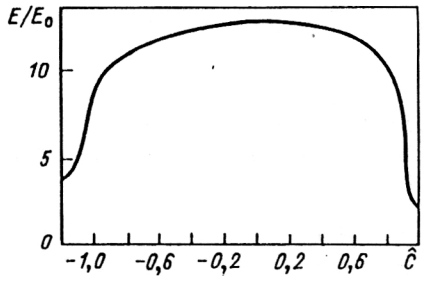

FIG. 28. Parameter variation. Dependence of the normalized field amplitude at the amplifier output in the high-efficiency regime on the normalized initial detuning. For zero initial detuning the amplifier efficiency is $\eta=40\%$, and the power gain on the undulator section with constant parameters is 40 dB.

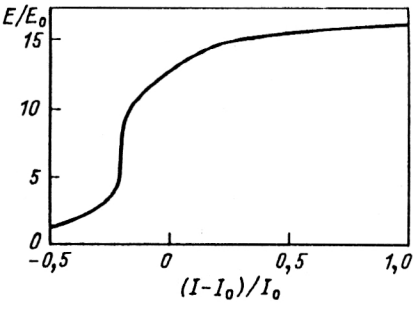

FIG. 29. Parameter variation. Dependence of the normalized field amplitude at the amplifier output in the high-efficiency regime on the change of the beam current. For $I=I_0$ the amplifier efficiency $\eta=40\%$, and the power gain on the undulator section with constant parameters is 40 dB.

under unity, these characteristics remain practically the same as in the low-efficiency regime. The dependence of the field amplitude at the amplifier output on the beam current for $\eta=40\%$ is shown in Fig. 29. We see that even for a significant increase of the current the output field amplitude is practically unchanged, and the amplifier efficiency is decreased only owing to the increase of the beam power. For example, when the beam current is raised by a factor of 1.5 with the other parameters of the problem fixed, the efficiency is decreased from 40 to 33%.

CONCLUSION

In this study we have systematically described the one-dimensional theory of the FEL amplifier. For this model to be applicable it is necessary that during the amplification process the radiation practically does not go outside the limits of the electron beam. This means that the wavelength of the radiation is small compared with the transverse dimensions of the electron beam. As a rule, the one-dimensional model gives a fairly good description of the FEL amplifier in the optical and ultraviolet regions. Moreover, the construction of the one-dimensional theory is also of great methodological importance as the first step in the development of complete three-dimensional models. The use of similarity techniques in constructing the theory not only makes the theory extremely clear and easy to understand, but it also provides a method of calculating the

TABLE I. The setup parameters.

The accelerator:	
electron energy, MeV	25
beam current, A	1000
energy spread, %	0.2
emittance, cm·rad	$2\pi\cdot 10^{-4}$
beam radius in the undulator, cm	0.13
The undulator:	
period, cm	4
field strength on the axis, G	1515
The master laser:	
wavelength of the radiation, μm	10.6
power, kW	1

TABLE II. The normalized parameters.

Rise parameter Λ_0, cm^{-1}	$3.1 \cdot 10^{-2}$
Space-charge parameter $\hat{\kappa}_p^2$	0.16
Energy-spread parameter $\hat{\Lambda}_T^2$	0.05
The parameter β	0.01

output characteristics of the amplifier which is very convenient for practical applications.

As an example, let us carry out the calculations for a FEL amplifier at a wavelength of 10.6 μm. The accelerator parameters are given in Table I.

The master laser on the given wavelength has a power of 1 kW and optimal focusing for the electron beam. We use a helical undulator with a period of 4 cm. From the synchronism condition (5) $C=0$, we uniquely obtain the required value of the magnetic field strength on the undulator axis: $H_0 = 1515$ G. The condition for the electron beam to match the undulator uniquely determines the radius of the electron beam. We therefore have all the needed characteristics and can calculate the dimensionless parameters of the problem. These are given in Table II.

Analysis of the parameters shows that in this case the influence of the space charge and the energy and angular spreads is small, so the calculations can be carried out using the equations for a "cold" electron beam, neglecting the space charge. Using the value of the normalized increment, $\sqrt{3}/2$, we find the increment of the power gain to be 23.3 dB/m. Using Eq. (24) and the graph in Fig. 1, we can obtain the values of the amplified power on the linear segment of the amplifier. We find that the linear stage of the amplification stops at a distance of about 160 cm from the beginning of the undulator. For the case of an undulator with constant parameters, Eqs. (50) and (48) can be used to determine the length at which saturation is reached and the efficiency of the amplifier in the saturation regime. For the case of an undulator with variable parameters, Eq. (55) gives the value of the coordinate where the variation begins, and Eq. (56) gives the law governing the variation of the field amplitude of the amplified wave as a function of the coordinate. Equation (53) can be used to calculate the change of the undulator period:

$$\lambda_0(z) = 4.0 \text{ cm} \quad \text{for} \quad z < 260 \text{ cm}, \quad \text{and}$$

$$\lambda_0(z) = (0.25 + 2.23 \cdot 10^{-4}(z - 260) + 1.73 \cdot 10^{-6}(z - 260)^2)^{-1} \text{ cm},$$

for $z > 260$ cm. At the end of the variation section ($z=430$ cm) the undulator period and the magnetic field strength are $\lambda_0 = 2.9$ cm and $H_0 = 2.1$ kG, respectively. Here the efficiency is increased to 10%. It is easy to check that in this example all the requirements for the one-dimensional model to be applicable are satisfied. The amplitude, current, and frequency characteristics can be calculated using the corresponding normalized graphs. In Table III we give the basic characteristics of the amplifier.

Of course, an efficiency greater than 10% can be attained, but then the conditions for the applicability of the one-dimensional model are violated and it becomes necessary to include diffraction effects, which lie outside the scope of the present study. Nevertheless, the calculation based on the one-dimensional model presented here is of practical interest and can be technically realized at the current level of development of accelerator technology.

In conclusion, we should note that, owing to limitations on the size of this study, we have consciously omitted one special point which is of practical interest. This is the study of systems with a longitudinal driving magnetic field. Here other types of instability can develop in addition to radiative instability, and the Coulomb instability of the negative mass of the longitudinal motion can be of particular interest from the practical point of view. Nevertheless, calculations carried out using the three-dimensional theory show that most cases of systems with a longitudinal field which can be realized in practice must be studied using the three-dimensional theory.

APPENDIX A. THE GENERAL FORM OF THE SOLUTION OF THE INITIAL-VALUE PROBLEM FOR A FEL AMPLIFIER WITH A COLD ELECTRON BEAM

In Sec. 1 we solved the initial-value problem using the Laplace method. In this Appendix we shall discuss a completely different method of solving this problem. When a cold beam is being analyzed, the kinetic equation (9) and the wave equation (13) can be reduced to a single differential equation for the field amplitude of the amplified wave $\tilde{E}$:

$$\tilde{E}''' + 2i\hat{C}\tilde{E}'' + (\hat{\kappa}_p^2 - \hat{C}^2)\tilde{E}' = i\tilde{E}, \tag{62}$$

where the prime denotes differentiation with respect to $\hat{z}$. Since Eq. (62) is a linear ordinary differential equation with constant coefficients, it is natural to seek a solution in the form

$$\tilde{E}(\hat{z}) = A \exp(\lambda \hat{z}).$$

According to Eq. (62), the factor λ in the argument of the exponential satisfies the algebraic equation

$$\lambda[(\lambda + i\hat{C})^2 + \hat{\kappa}_p^2] = i, \tag{63}$$

TABLE III. Output characteristics of the amplifier.

Linear amplification regime:	
undulator length, cm	160
gain, dB	27.9
frequency bandwidth of the amplification, %	3
Saturation regime (constant parameters):	
undulator length, cm	300
efficiency, %	1.4
gain, dB	55.2
frequency bandwidth of the amplification, %	3
Regime with parameter variation:	
total undulator length, cm	430
length of the segment with parameter variation, cm	170
efficiency, %	10
gain, dB	63.8
capture coefficient, %	65
frequency bandwidth of the amplification, %	3

which gives three values of λ determining three linearly independent solutions for the field amplitude:

$$\tilde{E}_1=\exp(\lambda_1\hat{z}),\quad \tilde{E}_2=\exp(\lambda_2\hat{z}),\quad \tilde{E}_3=\exp(\lambda_3\hat{z}).$$

To solve the initial-value problem we must know the three quantities

$$\tilde{E}(0),\quad \tilde{E}'(0),\quad \tilde{E}''(0),$$

which correspond to the field amplitude and its first and second derivatives with respect to $\hat{z}$ at the undulator input for $\hat{z}=0$. Then

$$\begin{pmatrix}\tilde{E}\\ \tilde{E}'\\ \tilde{E}''\end{pmatrix}_{\hat{z}}=M(\hat{z}|0)\begin{pmatrix}\tilde{E}\\ \tilde{E}'\\ \tilde{E}''\end{pmatrix}_0, \tag{64}$$

where the transition matrix $M(\hat{z}|0)$ is equal to

$$M=\begin{bmatrix}\tilde{E}_1 & \tilde{E}_2 & \tilde{E}_3\\ \tilde{E}_1' & \tilde{E}_2' & \tilde{E}_3'\\ \tilde{E}_1'' & \tilde{E}_2'' & \tilde{E}_3''\end{bmatrix}_z\times\begin{bmatrix}\tilde{E}_1 & \tilde{E}_2 & \tilde{E}_3\\ \tilde{E}_1' & \tilde{E}_2' & \tilde{E}_3'\\ \tilde{E}_1'' & \tilde{E}_2'' & \tilde{E}_3''\end{bmatrix}_0^{-1}.$$

The explicit expression for M has the form

$$M_{11}=\lambda_2\lambda_3B_1+\lambda_1\lambda_3B_2+\lambda_1\lambda_2B_3,$$

$$M_{12}=-(\lambda_2+\lambda_3)B_1-(\lambda_1+\lambda_3)B_2-(\lambda_1+\lambda_2)B_3,$$

$$M_{13}=B_1+B_2+B_3,\quad M_{21}=\lambda_1\lambda_2\lambda_3M_{13},$$

$$M_{22}=-\lambda_1(\lambda_2+\lambda_3)B_1-\lambda_2(\lambda_1+\lambda_3)B_2-\lambda_3(\lambda_1+\lambda_2)B_3,$$

$$M_{23}=\lambda_1B_1+\lambda_2B_2+\lambda_3B_3,\quad M_{31}=\lambda_1\lambda_2\lambda_3M_{23},$$

$$M_{32}=-\lambda_1^2(\lambda_2+\lambda_3)B_1-\lambda_2^2(\lambda_1+\lambda_3)B_2-\lambda_3^2(\lambda_1+\lambda_2)B_3,$$

$$M_{33}=\lambda_1^2B_1+\lambda_2^2B_2+\lambda_3^2B_3,$$

where to abbreviate the notation we have introduced

$$B_1=(\lambda_1-\lambda_2)^{-1}(\lambda_1-\lambda_3)^{-1}\exp(\lambda_1\hat{z}),$$

$$B_2=(\lambda_2-\lambda_1)^{-1}(\lambda_2-\lambda_3)^{-1}\exp(\lambda_2\hat{z}),$$

$$B_1=(\lambda_3-\lambda_1)^{-1}(\lambda_3-\lambda_2)^{-1}\exp(\lambda_3\hat{z}).$$

The quantities $\tilde{E}'$ and $\tilde{E}''$ at the undulator input are expressed in terms of the values of the complex amplitude of the first harmonic of the particle density in the phase space, f_1. Using the kinetic equation (9) and the wave equation (13), we have

$$\tilde{E}'(0)=\pi\theta_0c^{-1}\Lambda_0^{-1}j_1(0),$$

$$\tilde{E}''(0)=\pi\theta_0c^{-1}\Lambda_0^{-1}\tilde{j}_1'(0),\quad \tilde{j}_1(0)=\int f_1(0,P)dP,$$

$$\tilde{j}_1'(0)=-i\Lambda_0^{-1}\left[C\tilde{j}_1(0)+c^{-1}\gamma_z^{-2}\mathscr{E}_0^{-1}\omega\int f_1(0,P)PdP\right].$$

As an example, let us consider the case where an unmodulated electron beam and an electromagnetic wave of amplitude E_{ext} are fed to the amplifier input. The initial conditions for $z=0$ will be

$$\tilde{E}(0)=E_{\text{ext}},\quad \tilde{E}'(0)=0,\quad \tilde{E}''(0)=0.$$

According to (64),

$$\tilde{E}(\hat{z})=M_{11}(\hat{z}|0)E_{\text{ext}}.$$

This expression is identical to Eq. (23).

APPENDIX B. RAISING THE AMPLIFIER EFFICIENCY BY VARIATION OF THE UNDULATOR FIELD FOR CONSTANT PERIOD

In Sec. 3 we studied the method of raising the amplifier efficiency by varying the undulator period for constant magnetic-force parameter. Another method of raising the efficiency which is fairly easy technically is to vary the undulator field for constant period. It follows from the definition of the detuning parameter C that in order to preserve the synchronism in the bremsstrahlung of the particle beam, the undulator field H_0 must be decreased for constant period λ_0. The simplest method of variation is to have the field decrease as a quadratic polynomial:

$$\frac{H_0(z_i)-H_0(z)}{H_0(z_i)}=\varepsilon_0+\varepsilon_1(z-z_i)+\varepsilon_2(z-z_i)^2. \tag{65}$$

We introduce the normalized variables in the usual manner. Here the normalization factors are calculated from the initial values of the beam and undulator parameters. According to Eqs. (41) and (42), the normalized system of self-consistent field equations describing the interaction between the electron beam and the electromagnetic wave in the undulator with variation of the field at constant period has the form

$$\frac{d\hat{P}}{d\hat{z}}=\frac{1-[(1+\alpha)/\alpha]\,\beta T(z)}{1+\beta\hat{P}}\hat{\varphi}\cos(\psi+\psi_0),$$

$$\frac{d\psi}{d\hat{z}}=\frac{1}{(1+\beta\hat{P})^2}\left\{\hat{P}\left(1+\frac{\beta\hat{P}}{2}+T(\hat{z})\times\left(1-\frac{1+\alpha}{2\alpha}\beta T(\hat{z})\right)\right\}+\beta\hat{\varphi}\left(1-\frac{1+\alpha}{\alpha}\beta T(\hat{z})\right)\sin(\psi+\psi_0),\right. \tag{66}$$

$$\left.\begin{aligned}\frac{d\hat{\varphi}}{d\hat{z}}&=-\left(1-\frac{1+\alpha}{\alpha}\beta T(\hat{z})\right)\left[\frac{2}{N}\sum_{J=1}^{N}\frac{\cos(\psi_{(j)}+\psi_0)}{1+\beta\hat{P}_j}\right],\\ \frac{d\psi_0}{d\hat{z}}&=\frac{1}{\hat{\varphi}}\left(1-\frac{1+\alpha}{\alpha}\beta T(\hat{z})\right)\left[\frac{2}{N}\sum_{J=1}^{N}\frac{\sin(\psi_{(j)}+\psi_0)}{1+\beta\hat{P}_j}\right].\end{aligned}\right\} \tag{67}$$

The coefficients $\alpha=Q^2$ and $\beta=c\gamma_z^2\Lambda_0/\omega$ are calculated from the initial values of the beam and undulator parameters, and the function $T(z)$ is

$$T(\hat{z})=k_0+k_1(\hat{z}-\hat{z}_i)+k_2(\hat{z}-\hat{z}_i)^2,$$

$$k_0=\frac{\alpha\varepsilon_0}{\beta(1+\alpha)},\quad k_1=\frac{\alpha\varepsilon_1}{\beta\Lambda_0(1+\alpha)},$$

$$k_2=\frac{\alpha\varepsilon_2}{\beta\Lambda_0^2(1+\alpha)}. \tag{68}$$

At the beginning of the bremsstrahlung section, when the change in the particle energy is fairly small, we can expand in the small parameter $\beta\hat{P}$ in the equations of the system (66), (67). As a result, for low efficiency we have the following approximate system of working equations:

$$\frac{d\hat{P}}{d\hat{z}}=\hat{\varphi}\cos(\psi+\psi_0),\quad \frac{d\psi}{d\hat{z}}=\hat{P}+T(\hat{z}),$$

$$\frac{d\hat{\varphi}}{d\hat{z}}=-\hat{\rho}_1\cos(\psi_1-\psi_0),\quad \frac{d\psi_0}{d\hat{z}}=\frac{\hat{\rho}_1}{\hat{\varphi}}\sin(\psi_1-\psi_0),$$

which coincides with the system of equations (44), (45) describing the interaction between the particles and the wave in the undulator with variation of the period at Q = const in the low-efficiency approximation. Here the detuning parameter $\hat{C}(\hat{z})$ is equal to $T(\hat{z})$. Therefore, for $\eta\ll 1$ the two methods of varying the undulator parameters are physically equivalent.

The coefficients k_0, k_1, k_2, and $\hat{z}_i$ were selected using a program of optimizing to the field maximum for $(\hat{z}-\hat{z}_i)\gg 1$. The numerical modeling was carried out using the original system of equations (66), (67). The following values were obtained:

$$k_0=0,\quad k_1=1.44,\quad k_2=0.3,$$

$$\hat{z}_i=1.7+2(3)^{-1/2}\ln(E_0/E_{\text{ext}}).$$

The capture coefficient is 0.68. Let us now give a physical explanation of the fact that the value of the coefficient k_2 given here is somewhat less than the value of Sec. 3. The point is that during the initial bremsstrahlung section the captured particles undergo phase oscillations, and for $(\hat{z}-\hat{z}_i)\cong 3$ they come quite close to the boundary of the stability region. Owing to the increase of the amplitude of the wave field, the further bremsstrahlung of the particles proceeds in a more stable manner. Numerical modeling using the initial working equations (58), (59), and (66), (67) shows that as the undulator period decreases, the phase motion of the particles becomes more stable than the motion calculated from the approximate equations (44), (45), while, conversely, it is less stable when the undulator field is decreased. For parameters of practical interest $\alpha\cong 1$ and $\beta\cong 10^{-2}$ this difference is already significant, and for $k_2=0.36$ it causes the number of entrapped particles to decrease slightly in passing through the critical point. Therefore, the more stable regime for $k_2=0.3$ becomes optimal.

The length of the bremsstrahlung section (z_f-z_i) obviously cannot exceed the distance over which the undulator field H_0 decreases to zero as in (65), which can be found from the equation

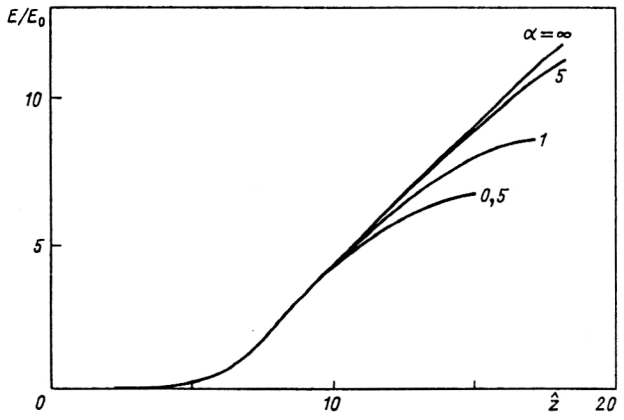

FIG. 30. Parameter variation. Dependence of the normalized field amplitude at the amplifier output on the normalized undulator length for various values of the parameter α. The parameter is $\beta=0.01$, $\hat{\kappa}_p^2=0$, and $\hat{\Lambda}_T^2=0$.

$$0.3\beta\frac{1+\alpha}{\alpha}\Lambda_0^2(z_f-z_i)^2$$

$$+1.44\beta\frac{1+\alpha}{\alpha}\Lambda_0(z_f-z_i)-1=0. \tag{69}$$

More precisely, the undulator field is bounded below not by zero, but by the condition $H_0\gg E/(2\gamma_z^2)$, according to which all the calculations we have carried out are valid with the assumption that the necessary transverse motion of the particles is determined by the undulator field, and not by the wave field. The normalized form of this condition using (65) and (68) is

$$\frac{1+\alpha}{\alpha}\beta^2\hat{\varphi}(\hat{z})\ll\left(1-\frac{1+\alpha}{\alpha}\beta T(\hat{z})\right). \tag{70}$$

In the numerical modeling this condition was enforced by the computer program, and the calculation was halted when the ratio of the left- and right-hand sides was 1:10. However, in the parameter range of practical interest,

$$0.1<\alpha,\quad \beta<0.03,$$

the length of the bremsstrahlung section found in this manner differs little from the length calculated using Eq. (69).

In Fig. 30 we show graphs of the function $\hat{\varphi}(\hat{z},\alpha,\beta)$ for α equal to 0.5, 1, and 5 and $\beta=0.01$ as a function of the normalized undulator length. For comparison, in the same figure we show the graph of the dependence $\hat{\varphi}(\hat{z})$ calculated using the approximate system of working equations (44), (45). In the calculation of all the graphs in Fig. 30 the normalized function describing the change of the undulator field $T(\hat{z})$ was chosen in the form

$$T(\hat{z})=1.44(\hat{z}-\hat{z}_i)+0.3(\hat{z}-\hat{z}_i)^2,\quad \hat{z}_i=1.7$$

$$+2(3)^{-1/2}\ln(E_0/E_{\text{ext}}).$$

We see from Fig. 30 that the larger the parameter α, the less the function $\hat{\varphi}(\hat{z},\alpha,\beta)$ deviates from linear behavior on the final bremsstrahlung section. The dependence of the maximum efficiency of the amplifier on the values of the

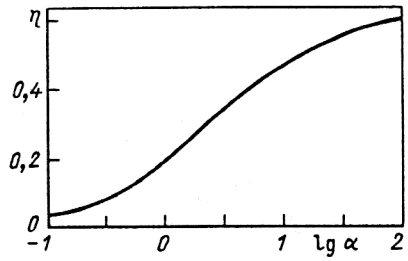

FIG. 31. Parameter variation. Dependence of the maximum amplifier efficiency on the parameter α for the parameter $\beta = 0.01$.

parameter α for $\beta = 0.01$ is shown in Fig. 31. We see that the deep stopping regime occurs for $\alpha \gg 1$, and in this case the method of varying the undulator field gives practically the same results as the method of varying the period with fixed magnetic-force parameter.

The numerical results show that the maximum efficiency of the amplifier depends weakly on the values of the parameter β, so that in the parameter range of practical interest, $0.003 < \beta < 0.03$, the graph in Fig. 31 can be used to determine the value of the maximum efficiency.

APPENDIX C. THE COMPUTATIONAL TECHNIQUE FOR A FEL AMPLIFIER WITH A FLAT UNDULATOR

All the results given above pertain to the case where the undulator of the FEL amplifier is helical, and the input radiation is circularly polarized. All the results of the numerical calculations and the corresponding graphs can be adapted to the case of linearly polarized radiation and a flat undulator, with a field of the form

$$H_y = 0, \quad H_x = H_\perp \cos(\kappa_0 z),$$

by the following redefinition of the parameters of the problem:

$$\Lambda_0 \to \Lambda_0' = [\pi j_0 \theta^2 \omega A_{JJ} \gamma^{-1} (\gamma_z')^{-2} I_A^{-1} (2c)^{-1}]^{1/3},$$

$$E_0 \to E_0' = 2\mathscr{E}_0 (\gamma_z')^2 (\Lambda_0')^2 c/(e\theta\omega A_{JJ}),$$

$$C \to C' = \kappa_0 - \omega(2c)^{-1}(\gamma_z')^{-2}, \quad \beta \to \beta' = c(\gamma_z')^2 \Lambda_0' \omega^{-1},$$

$$\kappa_p \to \kappa_p' = [4\pi j_0 \gamma^{-1} (\gamma_z')^{-2} I_A^{-1}]^{1/2},$$

$$\Lambda_T \to \Lambda_T' = 2^{-1/2} c^{-1} \omega (\gamma_z')^{-2} (\langle (\Delta\mathscr{E})^2 \rangle)^{1/2} \mathscr{E}_0^{-1}.$$

Here we have introduced the notation $\theta = eH_\perp/(\mathscr{E}_0 \kappa_0)$, and $(\gamma_z')^{-2} = \gamma^{-2} + \theta^2/2$. The coefficient A_{JJ} is determined from the expression $A_{JJ} = [J_0(g) - J_1(g)]^2$, where $g = \theta^2\omega/(8c\kappa_0)$; J_0 and J_1 are the Bessel functions of order zero and one. The field of the amplifier linearly polarized wave is described by the expression

$$E_x = 0, \quad E_y = E_p(z)\cos[\omega(z/c - t) + \psi_0(z)].$$

To demonstrate the method of calculating the characteristics of the FEL amplifier with a flat undulator, let us consider as an example the operation of the amplifier in the saturation regime. Proceeding in the manner described above, using (50) we find that right at resonance ($C' = 0$) in the absence of the space-charge and energy-spread effects

$$(\kappa_p'/\Lambda_0')^2 \to 0, \quad (\Lambda_T'/\Lambda_0')^2 \to 0,$$

the field of the wave reaches its maximum at a point a distance of

$$z_m = (\Lambda_0')^{-1}[3.1 + 2(3)^{-1/2} \ln(E_0'/E_p^{\text{ext}})]$$

from the beginning of the undulator, and this maximum is $(E_p)_{\max} = 2.34E_0'$. Here E_p^{ext} is the amplitude of the linearly polarized wave fed to the amplifier input.

We shall not discuss the derivation of the equations describing processes in an FEL amplifier with a flat undulator. If needed, the basic expressions for analyzing this problem can be found in Refs. 12 and 13.

[1)]FEL stands for free-electron laser.

[1] N. M. Kroll and W. A. McMullin, Phys. Rev. A **17**, 300 (1978).
[2] D. B. McDermott and T. C. Marshall, Phys. Quantum Electron. **7**, 509 (1980).
[3] E. Jerby and A. Gover, IEEE J. Quantum Electron. **QE-21**, 1041 (1985).
[4] L. D. Landau, Zh. Eksp. Teor. Fiz. **16**, 574 (1946) [in Russian].
[5] P. Sprangle, C. M. Tang, and W. M. Manheimer, Phys. Rev. A **21**, 302 (1980).
[6] C. M. Tang and P. Sprangle, J. Appl. Phys. **52**, 3148 (1981).
[7] C. M. Tang and P. Sprangle, Phys. Quantum Electron. **9**, 627 (1982).
[8] N. M. Kroll, P. L. Morton, and M. N. Rosenbluth, SRI Report JSR-79-01; IEEE J. Quantum Electron. **QE-17**, 1436 (1981).
[9] D. Prosnitz, A. Szoke, and V. K. Neil, Phys. Quantum Electron. **17**, 175 (1980); Phys. Rev. A **24**, 1436 (1981).
[10] P. Sprangle, C. M. Tang, and W. M. Manheimer, Phys. Rev. Lett. **43**, 1932 (1979).
[11] G. Bucholtz, *Calculation of Electric and Magnetic Fields* [in Russian] (IIL, Moscow, 1961).
[12] W. B. Colson, IEEE J. Quantum Electron. **QE-17**, 1417 (1981).
[13] M. Schmitt and C. J. Elliott, IEEE J. Quantum Electron. **QE-23**, 1552 (1987).
[14] R. Bonifacio, C. Pellegrini, and L. Narducci, Opt. Commun. **50**, 373 (1984).

Translated by Patricia A. Millard